Journal Pre-proof

Discovery of novel urea-diarylpyrazole hybrids as dual COX-2/sEH inhibitors with improved anti-inflammatory activity and highly reduced cardiovascular risks

Ahmed H. Abdelazeem, Asmaa G. Safi El-Din, Maha M. Abdel-Fattah, Noha H. Amin, Samir M. El-Moghazy, Mohammed T. El-Saadi

PII: S0223-5234(20)30634-6

DOI: https://doi.org/10.1016/j.ejmech.2020.112662

Reference: EJMECH 112662

To appear in: *European Journal of Medicinal Chemistry*

Received Date: 22 June 2020

Revised Date: 10 July 2020

Accepted Date: 11 July 2020

Please cite this article as: A.H. Abdelazeem, A.G. Safi El-Din, M.M. Abdel-Fattah, N.H. Amin, S.M. El-Moghazy, M.T. El-Saadi, Discovery Of Novel Urea-Diarylpyrazole Hybrids As Dual COX-2/sEH Inhibitors With Improved Anti-Inflammatory Activity And Highly Reduced Cardiovascular Risks, *European Journal of Medicinal Chemistry*, https://doi.org/10.1016/j.ejmech.2020.112662.

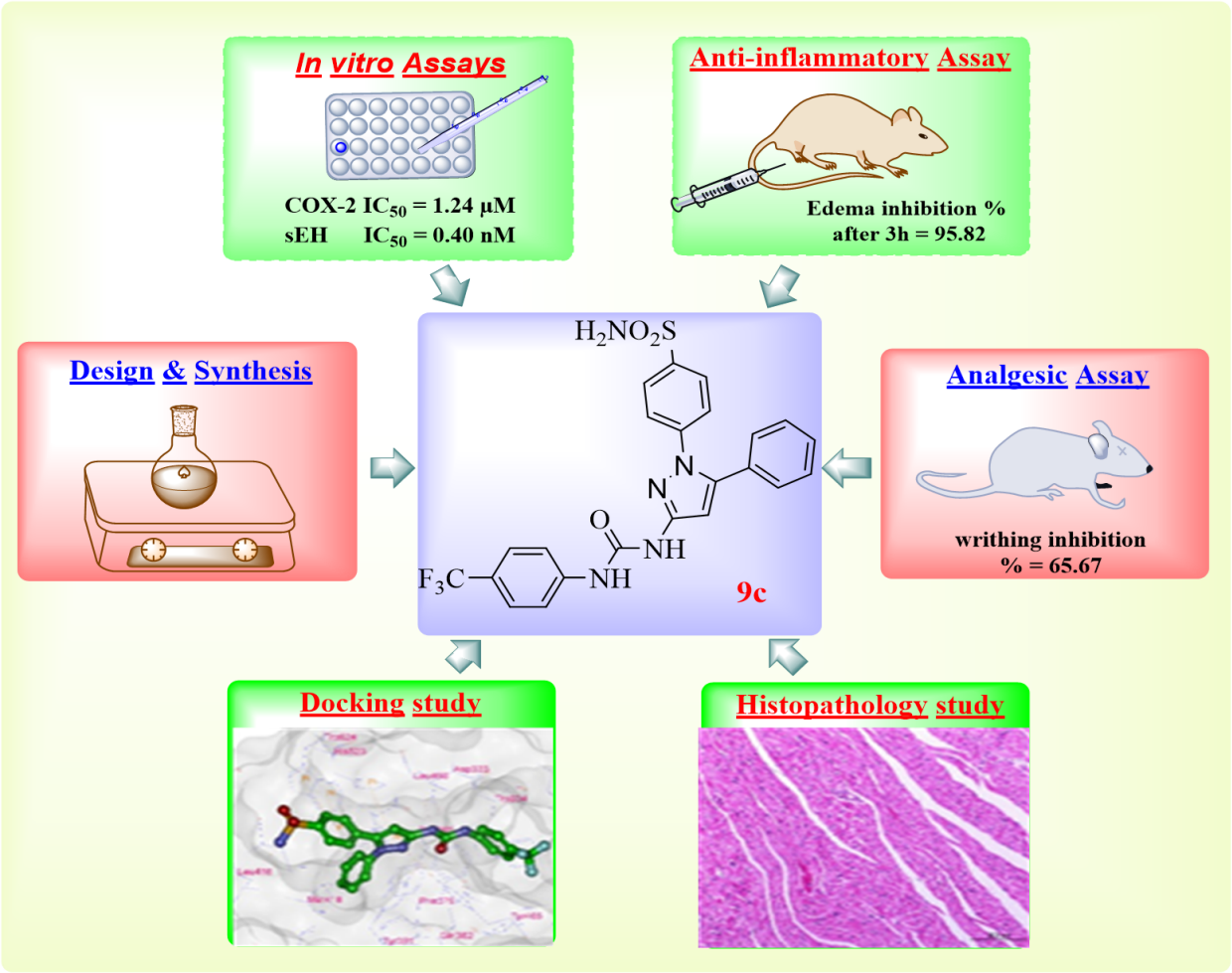
In vitro Assays
COX-2 IC50 = 1.24 µM
sEH IC50 = 0.40 nM
Anti-inflammatory Assay
Edema inhibition %
after 3h = 95.82
Design & Synthesis
H2NO2S
F3C
NH
O
NH
N
N
9c
Analgesic Assay
writhing inhibition
% = 65.67
Docking study
Histopathology study

Discovery Of Novel Urea-Diarylpyrazole Hybrids As Dual COX-2/sEH Inhibitors With Improved Anti-Inflammatory Activity And Highly Reduced Cardiovascular Risks

Ahmed H. Abdelazeem[1,*]; Asmaa G. Safi El-Din[1]; Maha M. Abdel-Fattah[2]; Noha H. Amin[1]; Samir M. El-Moghazy[3*]; Mohammed T. El-Saadi[1, 4]

[1]Department of Medicinal Chemistry, Faculty of Pharmacy, Beni-Suef University, Beni-Suef 62514, Egypt; [2]Department of pharmacology and Toxicology, Faculty of pharmacy, Beni-Suef University, Beni-Suef 62514, Egypt; [3]Department of Pharmaceutical Chemistry, Faculty of Pharmacy, Cairo University, Cairo 11562, Egypt; *[4]Department of Medicinal Chemistry, Faculty of Pharmacy, Sinai University, Qantara, Egypt.*

**To whom correspondence should be addressed:*

Ahmed H. Abdelazeem, Ph.D. Department of Medicinal Chemistry, Faculty of Pharmacy, Beni-Suef University, Beni-Suef 62514, Egypt.

E-mail address: ahmed.abdelazeem@pharm.bsu.edu.eg

Samir M. El-Moghazy, Ph.D. Department of Pharmaceutical Chemistry, Faculty of Pharmacy, Cairo University, Kasr-El-Eini Street, 11562 Cairo, Egypt.

E-mail address: samirelmoghazy@gmail.com

Graphical Abstract:

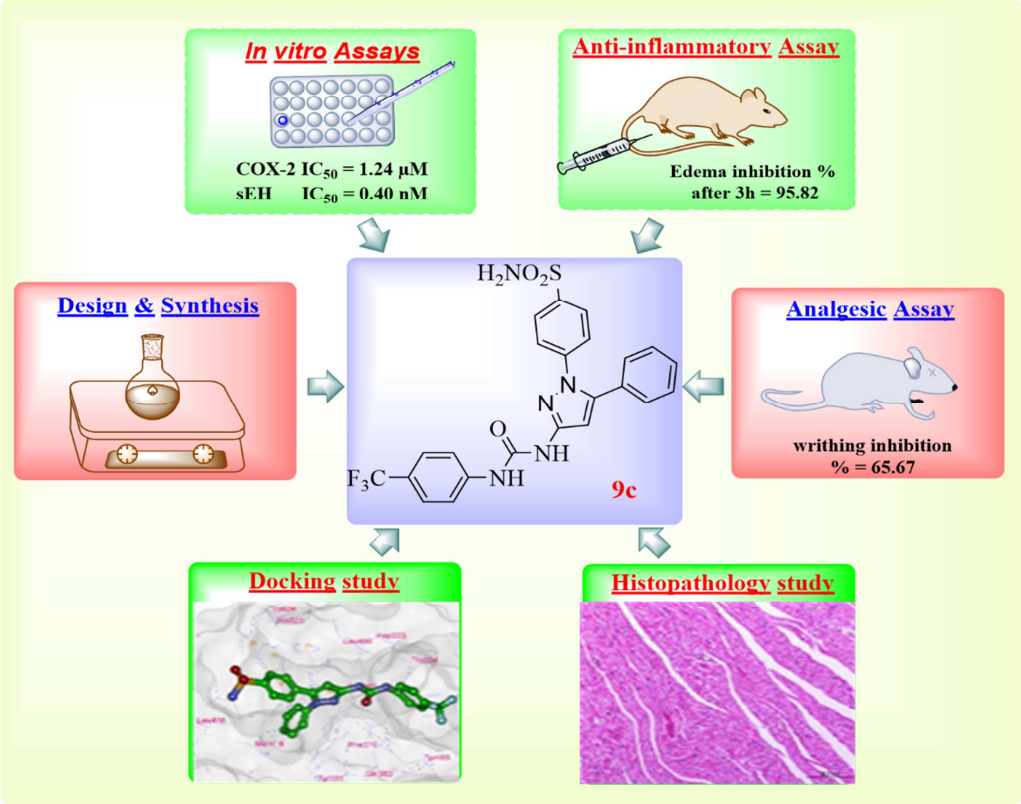

ABSTRACT:

Herein we describe our efforts to develop novel anti-inflammatory/analgesic agents devoid of known cardiovascular drawbacks. In doing so, two 1,5-diarylpyrazole series of urea linked (**9a-f**) and amide linked (**11a-f)** compounds were synthesized and evaluated *in vitro* as dual COX-2/sEH inhibitors using recombinant enzyme assays. The *in vivo* anti-inflammatory and analgesic activities were then examined using reported animal models. Compounds **9b** and **9c** showed the highest inhibitory activities against both COX-2 and sEH (IC_{50} of COX-2 = 1.85 and 1.24 µM; sEH = 0.55 and 0.40 nM, respectively), besides showing the best activity as anti-inflammatory agents. Interestingly, the cardiovascular profile of the two compounds **9b** and **9c** was evaluated through measuring some biochemical parameters such as prostacyclin (PGI_2), lactate dehydrogenase (LDH), troponin-1 (Tn-1), tumor necrosis factor- α (TNF-α), creatine kinase-M (CK-M) and reduced glutathione (GSH) in addition to a histo-pathological study to investigate the changes in the heart muscle. The results confirmed that compounds **9b** and **9c** have a more favorable cardio-profile than celecoxib with much less cardiovascular risks associated with the common selective COX-2 inhibitors. Finally, the current work provided a promising approach that can be optimized to serve as a lead project to overcome the cardiovascular toxicity related to the traditional selective COX-2 inhibitors.

Keywords: 1,5-Diarylpyrazole; Dual COX-2/sEH; sEH inhibitor; Cardiotoxicity, Anti-inflammatory.

1. Introduction:

For many years, the arachidonic acid (AA) cascade mediators have been focused on the therapy of several medical conditions including inflammation, pain, cancer, asthma and cardiovascular disorders [1–8]. It is well established that the primer step of the AA cascade is its release from the cellular membrane under the effect of the phospholipase A_2 (PLA_2) [4,5,9]. In consecutive steps, AA is bio-converted by several specific oxygenases to pro-inflammatory, pro-resolving in addition to anti-inflammatory mediators [10,11]. The inhibition of these specific oxygenases blocks their output mediators release, hence they can be utilized in many kinds of pharmaceutical researches and conditions [12]. For instance, cyclooxygenase inhibitors (COX pathway), are broadly used in the treatment of inflammatory diseases, exemplified by celecoxib, rofecoxib and valdecoxib [5,9,13]. On the other hand, zileuton, the drug of choice for allergy treatment, acts through the inhibition of lipoxygenase (LOX pathway; the second pathway of arachidonic acid cascade metabolism) as shown in **Fig. 1** [9,13,14].

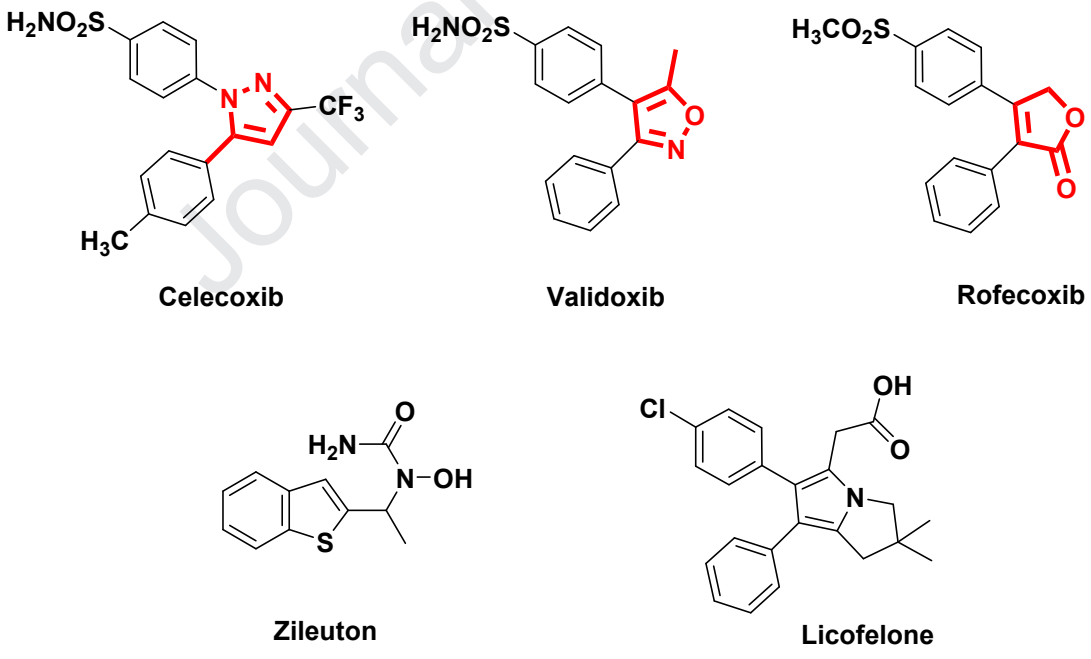

Fig. 1. Some known inhibitors of COX-2 and 5-LOX enzymes

Traditional non-steroidal anti-inflammatory drugs (NSAIDs) were considered the first pivot of inflammation treatment due to its ability to put down prostaglandins (PGs), the prominent prostanoids associated with several biological and pathological functions [15]. Unfortunately, their long-term use

was well-known to be accompanied by severe gastrointestinal toxicity as a consequence of their COX-1 inhibition, the enzyme responsible for generation of the gastro-protective prostaglandin E_2 (PGE_2) [16]. Accordingly, improvement of selective COX-2 inhibitors was considered as a promising approach that circumvents NSAIDs-gastrointestinal injury adverse effects. However, the appearance of a novel side adverse effect, cardio-toxicity, lead to the rebound of some selective COX-2 inhibitors from clinical fields [17]. The incidence of thrombotic cardiovascular disorders caused by COX-2 inhibitors were primarily due to the imbalance in the ratio of the thromboxane A_2 (TX A_2; vasoconstrictor/prothrombotic agent via action thromboxane-A synthase) to prostacyclin (PGI_2; vasodilator/anti-aggregative agents synthesized via the action of COX-2) levels [18,19]. This serious episode had a resounding effect which proved the need for developing new selective COX-2 inhibitors with a better cardiovascular profile. Recently, great attention has been devoted to the third arachidonic acid metabolic pathway (cytochrome P450) which involves release of vasoconstrictive/pro-inflammatory 20-hydroxyeicosatetranoic acid (20-HETE) and epoxy-eicosatrienoic acids (EETs) [20,21] as shown in **Fig. 2**.

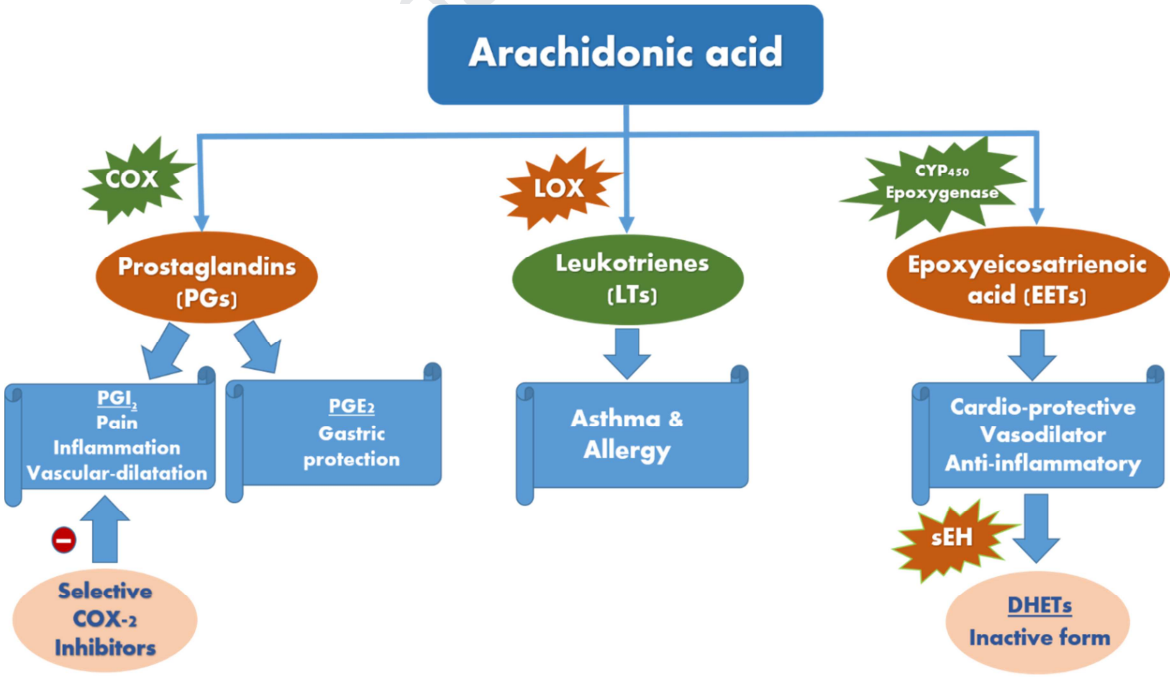

Fig. 2. The arachidonic acid metabolism pathways

EETs are known as effective contributors to modulate numerous homeostatic biological process including: inflammation [22,23], pain [24,25], vascular reactivity [26], blood pressure [27] as well as cardiovascular protective features [28,29]. It was reported that the cardioprotective activity of EETs are exhibited by several mechanisms including vasodilation of coronary vessels via stimulation of endothelial calcium-activated potassium channel (Kca) [30]. Moreover, EETs showed pro-angiogenic properties that is associated with cardioprotection in chronic phases through the EET-peroxisome proliferator activated receptor γ (PPARγ) pathway [31]. However, EETs are metabolized into pro-inflammatory dihydroxy eicosatrienoic acids (DHETs) by the action of soluble epoxide hydrolase enzyme (sEH), **Fig. 2** [32].

Accordingly, the inhibition of sEH has been proposed as a novel therapeutic approach for treatment of numerous biological disorders including pain, inflammation, hypertension and cardiovascular disorders depending on its ability for preserving the advantageous effects of EETs through enhancing their levels in the plasma and biological tissues [33–37]. Despite the various developed sEH inhibitors (e.g. AUDA, CDU, AUCB and TPAU), no sEH inhibitor has been presented to the market yet. Only some hopeful sEH inhibitor candidates are subjected now to clinical trials such as GSK2256294A in Phase-I and AR9281 in Phase-II against chronic obstructive pulmonary disease (COPD) and hypertension[38–40], as shown in **Fig. 3**.

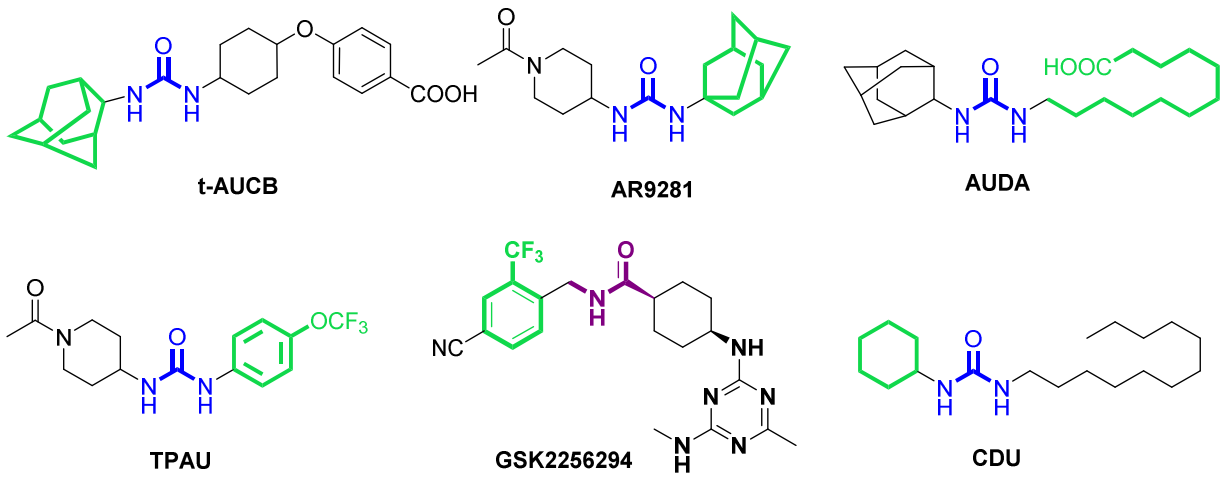

Fig. 3. Some reported sEH inhibitors with high potency in nanomolar range

In particular, hybridization of inhibitors of COX-2 and sEH enzymes has been proposed for the development of a harmonious target as an anti-inflammatory agent by poly-pharmacology technique. The amalgamation of selective COX-2 inhibitor and sEH inhibitor has been proved to act as a dual synergistic effect that caused reduction of both inflammation and cardiovascular risks [41]. This hypothesis was illustrated by several mechanisms including ability of COX-2/sEH combination to decrease PGE_2 without any change in PGI_2/TXA_2 ratio due to up-regulation of PGI_2 synthases, the enzyme responsible for producing PGI_2 [41,42]. Subsequently, COX-2/sEHI combination will allow to reduce COX-2 dose and concomitant dose-dependent cardiovascular adverse effects [43].

Based on the aforementioned studies, it was conceptualized that the development of novel dual inhibitors of COX-2 and sEH would be a promising approach to resuscitate COX-2 inhibitors with an overall successful outcome of both anti-inflammatory treatment for ulcer patients and profound safety margins against cardiovascular risks.

Rational design:

One of the most important drug design approaches used to reduce drug toxicity and improve biological activity is multi-target-directed ligand (MTDL) technique carried out by the covalent conjugation of various active moieties (pharmacophores) having different mechanisms of actions, yet with precise pharmacophoric selection for each individual target. Based on this concept, the design of our newly suggested COX-2/sEH dual inhibitors depends on finding two pharmacophores to hit the both targets concurrently with maintaining good pharmacodynamic and pharmacokinetic profiles.

Celecoxib- and SC-558-based pharmacophore was placed as the first part in our strategy for targeting COX-2 enzyme since it contains all the required COX-2 pharmacophoric moieties including Y-shaped structure (diaryl-heterocycles) with a sulfonamide group at the *p*-position of one of the two phenyl rings. Moreover, the presence of adjacent five-membered heterocyclic core, a pyrazole ring, which has been critical for high activity.

Exploring the sEH pharmacophoric moieties to build the second part in our newly suggested dual ligands was extracted from the study of critical interactions and the positioning of known selective sEH inhibitors inside the catalytic domain of its 3D protein structure. Consequently, this investigation revealed that the substituted urea or amide moieties were found to be essential chemical entities involved in these interactions and important for the whole activity [40]. This was clear in several reported sEH inhibitors such as AR9281, AUDA and GSK2256294. Additionally, some other substituents including trifluoromethyl aniline, cyclohexyl, adamantyl, piperidine and long chain dual amine/fatty acid have been pointed as secondary pharmacophoric moieties that significantly contribute in the sEH potency [40]. Taking these bullets into our consideration, we have combined the structural features of both COX-2 and sEH pharmacophores into one hybrid scaffold as depicted in **Fig. 4**.

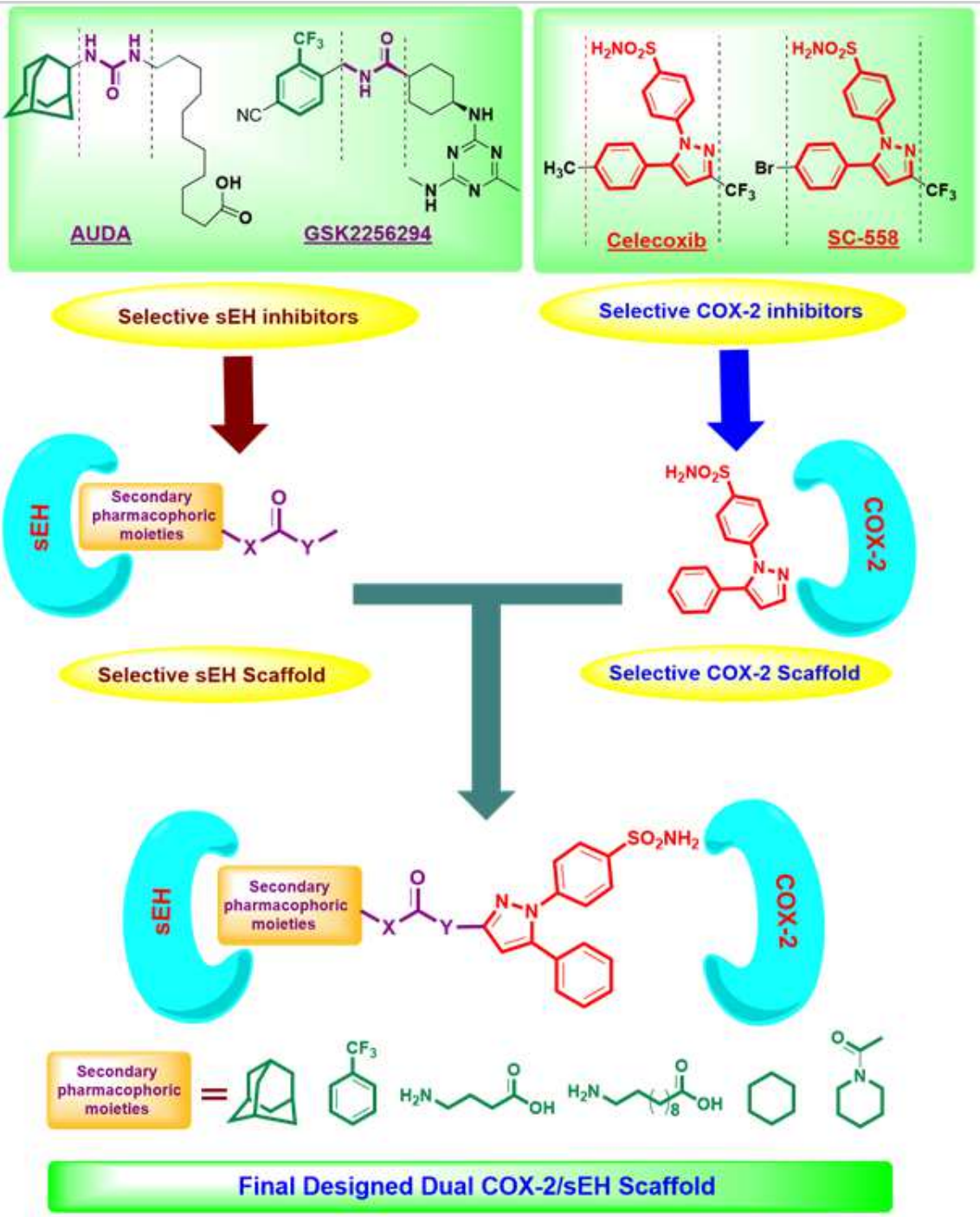

Fig. 4. The design strategy of our newly designed dual COX-2/sEH scaffold

2. Results and discussion:

2.1. Chemistry:

In the present study, the novel pyrazole-based derivatives were synthesized as represented in **Scheme 1**. The β-diketone **2** was prepared by condensation of acetophenone **1** and diethyl oxalate (Claisen Condensation) as reported [44]. The (4-aminosulfonyl) phenyl hydrazine hydrochloride (**4)** was obtained by diazotization of sulfanilamide **3**, followed by reduction of the diazonium salt with tin (II)

chloride [45]. The regio-selective cyclization of β-diketone **2** with hydrochloride salt of phenyl hydrazine **4** in ethanol to afford the 1,5-diarylpyazole compound **5** according to Knorr pyrazole synthesis method was adopted [46]. The hydrazide intermediate **6** was furnished by reacting 1, 5-diarylpyrazol ester **5** with hydrazine hydrate under reflux as reported [47].

Scheme 1:

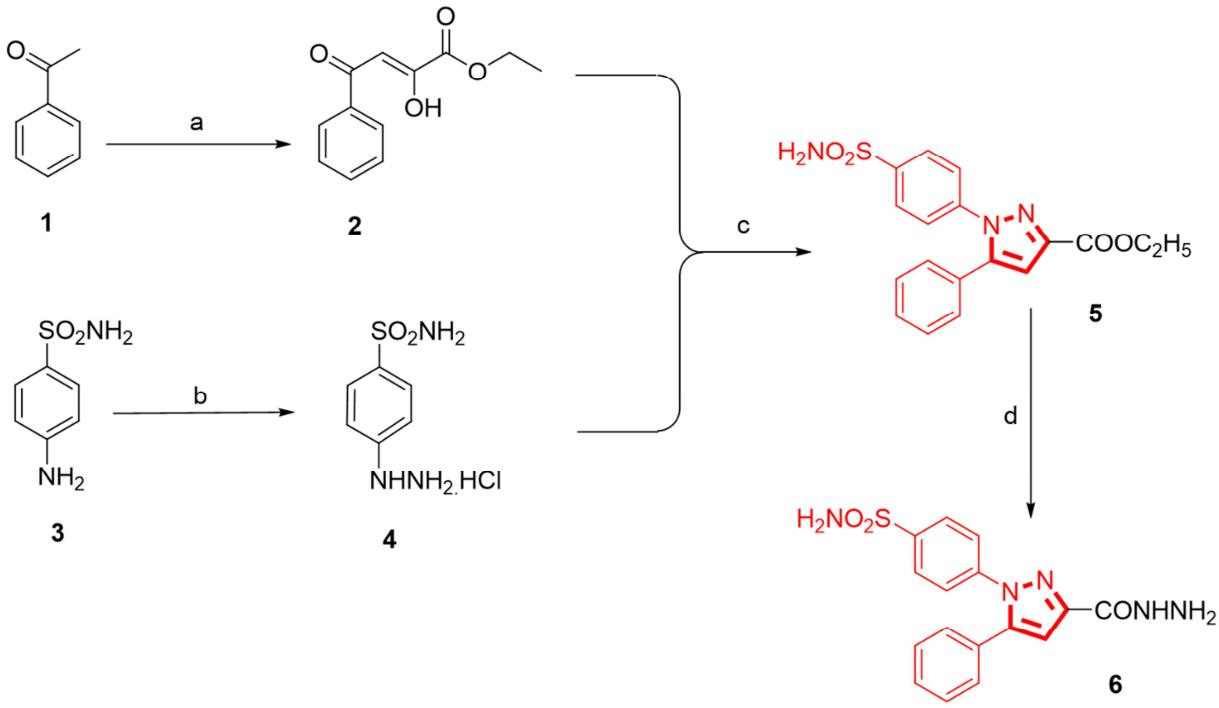

Scheme 1. The synthesis of compound 6. Reagents and reaction conditions: a) Diethyl oxalate, EtO^-Na^+, EtOH, rt, overnight; b) i. $NaNO_2$/ HCl, 0-5 ^oC, ii. $SnCl_2$/ HCl, overnight, refrigerator; c) EtOH, reflux, 12 h; d) $NH_2NH_2.H_2O$, EtOH, reflux at 80 ^oC, 6 h (65%).

The acyl azide **7** was prepared by the reaction of hydrazide **6** with *in situ* generated nitrous acid, then simultaneously was undergone Curtius rearrangement as outlined in **Scheme 2**. The Curtius rearrangement allowed the intra-molecular transformation of acyl azide **7** into isocyanate intermediate **8** through reflux in toluene. Consecutively, the isocyanate was treated *in situ* with aliphatic primary, secondary amine or amino acids in the presence of pyridine to obtain derivatives of urea. The proposed chemical structure of these derivatives was confirmed by their spectral data, where ^1H NMR of compound **9a** was confirmed by the appearance of two single peaks of two NH at δ 9.00 and 6.69 ppm, in addition to the characteristic peaks of cyclohexyl at range δ 1.17-3.55 ppm. ^{13}C NMR

spectrum showed signals at δ 22.99, 23.77, 33.17, and 48.17 ppm assigned to the characteristic cyclohexyl carbons.

Scheme 2:

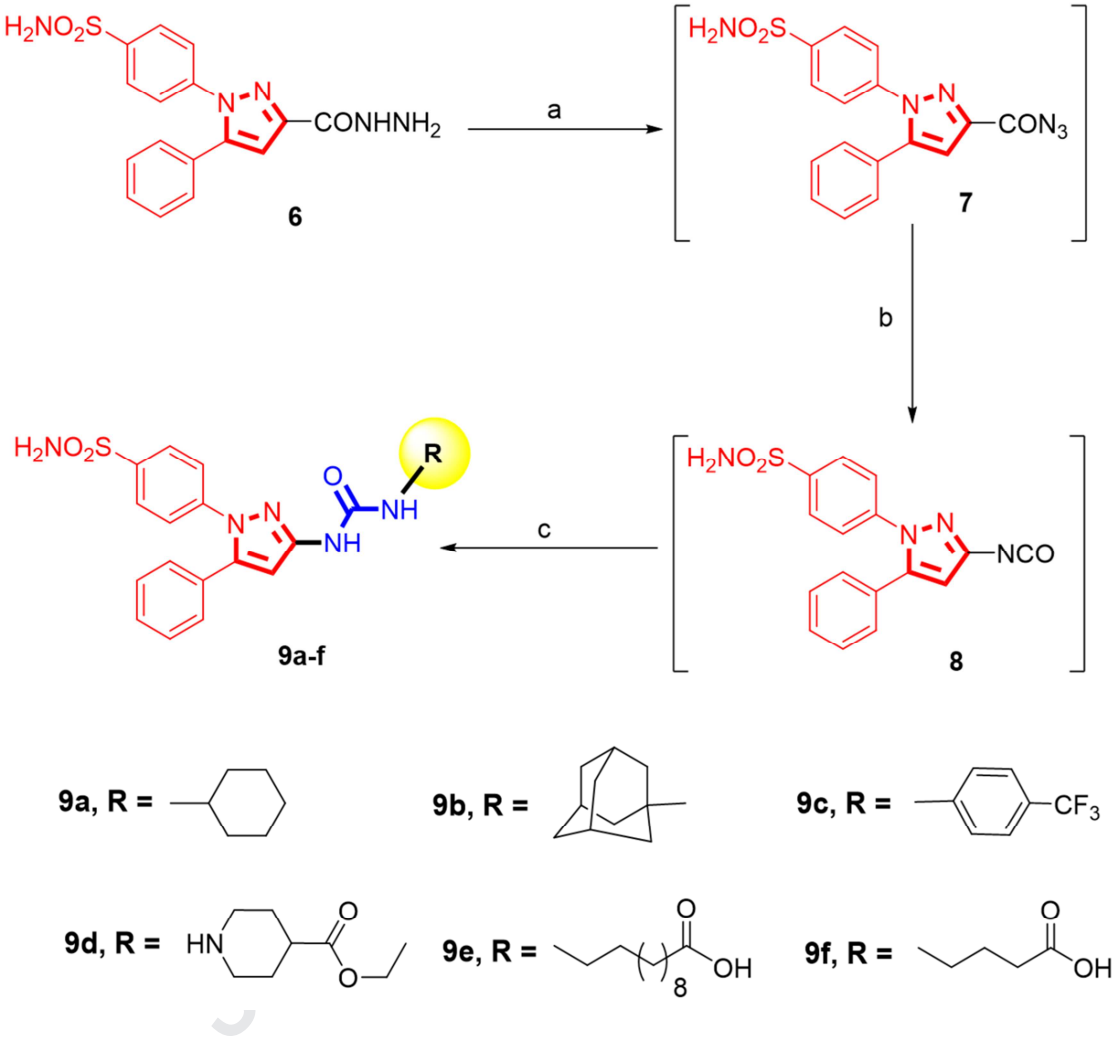

Scheme 2. The synthesis of compounds 9a-9f. Reagents and reaction conditions: a) $NaNO_2$/ HCl, 0-5 C; b) Toluene, reflux at 110-115 ^oC, 0.5h; c) appropriate amine, pyridine, reflux, 24 h (51-63%).

Regarding the amide derivatives **11a-f**, they were synthesized through the formation of the corresponding acyl chlorides. The acid of pyrazole **10** was synthesized through ester saponification by heating with KOH in methanol [48] followed by treating with thionyl chloride under reflux in the presence of drops of dimethylformamide for 3h. A simple condensation reaction was undergone between the reactive intermediates acyl chlorides and different amines to afford the target 1, 5-disubstituted pyrazol-3-carboxamide **11a-f** as described in **Scheme 3**. The postulated compounds

were confirmed by their IR, NMR and mass spectral data. Evidence for the formation of compounds **11a-f** was supported by ^{1}H NMR spectrum and revealed the characteristic peaks of the attached amine at their specific signals. ^{1}H NMR of compound **11c** showed the characteristic peaks of triflouromethyl aniline at δ 8.01-7.24 ppm in addition of another peak at δ 10.16 ppm attributed to the amide NH group where it disappeared upon deuteration. Also, ^{13}C NMR revealed the peak of amide at 160.53 ppm.

Scheme 3:

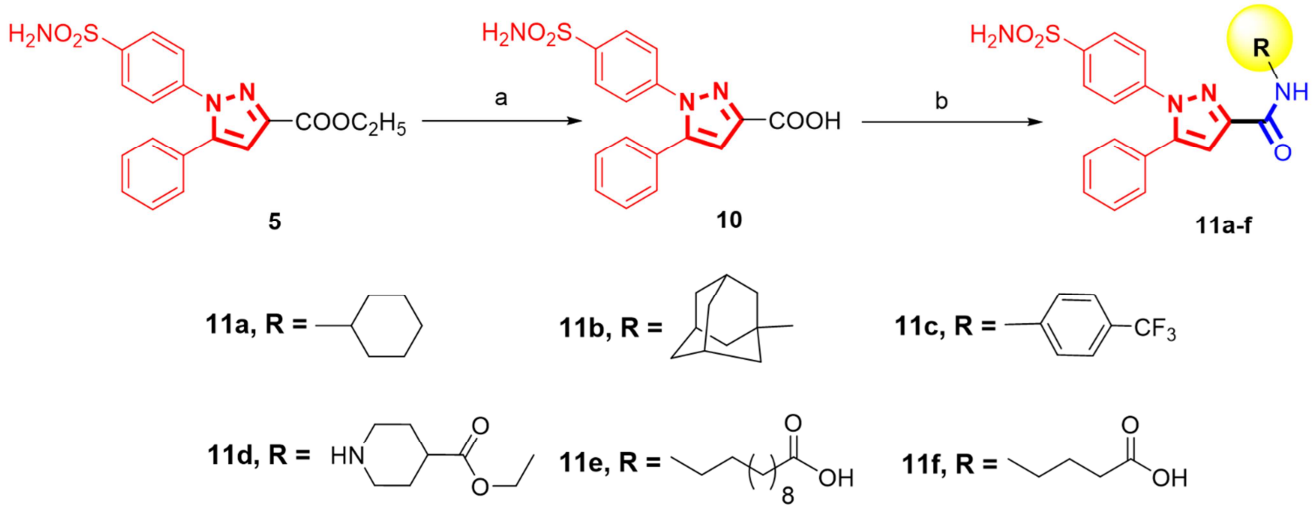

Scheme 3. The synthesis of compounds 11a-11f.Reagents and reaction conditions: a) KOH, MeOH, reflux at 65 ^{o}C, 12 h; b) i. $SOCl_2$, DMF, reflux, 3h ii) appropriate amine, TEA, CH_2Cl_2, rt, overnight (45-85%).

2.2. Pharmacology:

2.2.1. *In vitro* COXs/sEH assays:

Evaluation of all synthesized compounds for their *in vitro* inhibition of human COX-1/COX-2 enzymes using enzyme immunoassay (EIA) kits and human sEH enzyme using a cell-based assay kit was carried out by measuring IC_{50} (The concentration causing 50% enzyme inhibition). Moreover, in case of *in vitro* COX-1/COX-2 assay, the selectivity of these compounds is another efficacy index, where it could be estimated as COX-1 IC_{50}/COX-2 IC_{50}. The obtained results of both IC_{50} and selectivity were listed as shown in **Table 1**. The tested compounds results showed good COX-2 inhibitory activity (IC_{50} = 1.24-4.12 μM) and selectivity index (*SI*) values between 2.85 and 7.03

compared to celecoxib (IC_{50} = 0.95 μM; SI = 6.44) as selective COX-2 inhibitor reference. On the other hand, all the compounds showed moderate inhibitory activity against sEH with IC_{50} range 0.98–4.00 nM comparing to AUDA (IC_{50} = 0.49 nM) as a sEH inhibitor reference except two compounds **9b** and **9c** which elicited good sEH inhibition with IC_{50} of 0.55 and 0.40 nM respectively. Obviously, the results revealed that the compounds possessing a urea linker (**9a-f)** were more potent as selective COX-2 inhibitors (IC_{50} = 1.24-2.89 μM range) and sEH inhibitors (IC_{50} = 0.40-4.01 nM) corresponding to amide linker as shown in compounds **11a-f** (COX-2 IC_{50} = 2.05-4.12 μM range; sEH IC_{50} = 1.15-2.38 nM). Moreover, compounds **9a-c** showed the highest selectivity index among the tested compounds towards COX-2 (in range of 5.23-7.03) and the highest potency against sEH with IC_{50} of 0.98-0.44 nM, in order of **9c** > **9b** > **9a**. Obviously, 4-(1-phenyl-3-(3-(4-(trifluoromethyl)phenyl) ureido)-1*H*-pyrazol-5-yl)benzenesulfonamide (PTPUP) **9c,** which possessed a *p*-triflouromethyl anilinyl moiety directly attached to urea linker, was the most potent dual COX-2/sEH inhibitor with (COX-2, IC_{50} = 1.24 μM; *SI* = 7.03; sEH, IC_{50} = 0.40 nM).

Table 1: *In vitro* COX-1\COX-2 and sEH inhibition results of the newly synthesized compounds **9a-f**, **11a-f**, celecoxib and AUDA as a reference drug.

Compound code	COX Inhibition (IC_{50} μM)		Selectivity Index[a]	sEH inhibition (IC_{50} nM)[b]
	COX-1	COX-2		
9a	10.62	2.03	**5.23**	**0.98±0.013**
9b	11.85	1.85	**6.41**	**0.55±0.009**
9c	8.72	1.24	**7.03**	**0.40±0.011**
9d	10.1	2.89	3.49	1.74±0.025
9e	10.92	2.18	5.01	1.57±0.015
9f	9.87	1.99	4.96	4.01±0.012
11a	10.22	2.48	4.12	2.38±0.041
11b	8.99	2.15	4 .18	1.15±0.029

11c	9.12	2.05	4.45	1.21±0.011
11d	11.74	4.12	2.85	1.61±0.037
11e	10.54	3.04	3.47	3.31±0.037
11f	12.75	4	3.19	1.84±0.022
Celecoxib	6.12	0.95	6.44	**261.14±15.1**
AUDA	----	----	----	**0.49±0.009**

[a]*Selectivity index was calculated by dividing COX-1 IC_{50} by COX-2 IC_{50})*

[b]*The values are the mean ± SEM (n = 3)*

The reference drugs and the most active compounds results were written in Bold

2.2.2. *In vivo* Evaluation:

2.2.2.1. *Analgesic activity:*

Acetic acid-induced writhing method [49] was applied to evaluate the analgesic activity of all the tested compounds. The efficacy of the targeted compounds was determined through calculating the reduction in the number of acetic acid-induced writhing episodes and hence detecting their potency. The detected results were outlined in **Table 2**. The results exposed that all the compounds exhibited moderate analgesic activity with % inhibition in the number of writhing range between 22.38-65.67%, if compared to the reference drug, celecoxib with 13.43%. Interestingly enough, compound **9c**, the most potent *in vitro* dual COX-2/sEH inhibitor, elicited also the highest analgesic activity among the rest of other compounds (% inhibition = 65.67 %; Potency = 4.88).

Table 2: Results of analgesic activity of the new compounds **9a-f** and **11a-f** using acetic acid-induced writhing assay in mice compared to celecoxib.

Compound code	No. of writhes in 5–15 min after treatment [a] (Mean±SE)	% Inhibition	Potency[b]
9a	23.50±0.2	29.85	2.23
9b	25.25±0.7	24.62	1.83
9c	**11.50±0.6**	**65.67**	**4.88**
9d	20.75±0.3	38.05	2.83

9e	23.00±0.3	31.34	2.33
9f	20.25±0.7	39.55	2.94
11a	23.00±0.4	31.34	2.33
11b	12.50±0.4	62.68	4.66
11c	19.25±0.4	42.53	3.16
11d	24.50±0.6	26.86	2
11e	22.25±0.6	33.58	2.5
11f	26.00±0.6	22.38	1.66
Celecoxib	29.00±0.6	**13.43**	**1**
Control	33.50±0.8	--	--

[a]*Values are given as mean ± SE*

[b]*Potency are calculated according to equation of relative potency % = % of inhibition of tested compound / % of inhibition of control X 100*

Celecoxib and the most active compounds results were written in Bold

2.2.2.2. Anti-inflammatory activity:

The anti-inflammatory activity of the tested compound was determined using carrageenan-induced rat paw edema method [50]. The efficacy of the compounds was expressed as the decrease in edema paw volume and calculated % edema inhibition (EI %) after 1, 3 and 5 h compared to standard celecoxib drug, **Table 3**. The results elicited that all the compounds showed wide range in edema inhibition percentages after the three-time intervals 1, 3 and 5 hours. After 1 hour, all compounds showed weak to moderate EI% in range 28.18-78.73% comparing with celecoxib 81.17%. Meanwhile, after 3 hours, EI% of all compounds was increased to reach to the range of 57.18-95.82% in contrast to celecoxib whose EI% slightly increased to become 82.71%. Finally, after 5 hours, the increase in EI% was continued to be recorded in the range of 69.87-98.15% in comparison with celecoxib which showed EI% of 88.30%. Using 5 hours results as a criterion for the comparison, all compounds showed lower anti-inflammatory activity than celecoxib except compounds **9a-c** that showed the highest EI% among all compounds in addition to celecoxib (EI% = 98.15-88.76% for **9a-c**; EI% = 88.30% for celecoxib). The aforementioned results concluded that compound **9c** elicited the highest

anti-inflammatory activity among all the rest of the compounds with EI % = 98.15 in comparison with celecoxib EI % = 88.30 at the same time interval.

Table 3: Results of anti-inflammatory activity of synthesized compounds **9a-f** and **11a-f** using carrageenan-induced rat paw edema model in rats compared to celecoxib.

Compound code	Change in paw volume in (mm) after drug digestion(±SEM)			Anti-inflammatory activity (Edema inhibition %)		
	1h	3h	5h	1h	3h	5h
9a	3.48±0.16	3.17±0.01	2.19±0.07	**78.73**	**81.35**	**88.76**
9b	0.08±6.18	0.31±1.08	0.11±1.21	**62.22**	**92.02**	**93.79**
9c	0.21±5.88	0.27±0.71	0.03±0.36	**64.06**	**95.82**	**98.15**
9d	0.16±10.81	0.60±6.84	0.35±4.92	33.92	59.76	74.74
9e	5.44±0.14	5.52±0.10	4.40±0.3	66.75	67.53	77.41
9f	0.29±9.40	0.28±4.68	0.17±4.92	42.54	72.47	74.74
11a	0.36±11.28	0.27±7.28	0.22±4.92	31.05	57.18	74.74
11b	0.36±9.48	0.51±.3.99	0.760±3.08	42.05	76.53	84.19
11c	0.97±6.03	0.64±4.28	0.4202.58	63.14	74.82	86.76
11d	0.18±10.68	0.23±6.18	0.09±5.87	34.72	63.65	69.87
11e	6.73±0.31	7.28±0.35	5.34±0.16	58.86	57.18	72.59
11f	0.51±11.75	0.21±5.76	0.19±5.87	28.18	66.12	69.87
Celecoxib	3.08±0.15	2.94±0.08	2.28±0.14	**81.17**	**82.71**	**88.3**
Control	0.24±16.36	17.00±0.28	19.48±0.26	--	--	--

The edema inhibition % is calculated according to the following equation:

EI(%) = (1-W_t/W_c) x 100 where W_t symbolized the main increase in the tested compound groups paw thickness and W_c symbolized the mean increase in control group paw thicknesses.

The results analyzed by ANOVA (n = 4), P < 0.05 were all significant from the control.

Celecoxib and the most active compounds were written in Bold

2.2.2.3. Cardiovascular Evaluation:

The possible cardiovascular risks of the most active compounds **9b** and **9c** was evaluated using the celecoxib induced cardio-toxicity in rats as reported [51,52]. The response of the heart towards the tested compounds was expressed as the change in biochemical parameters obtained from both sera

including lactate dehydrogenase (LDH), troponin-I (Tn-I), tumor necrosis factor-α (TNF-α), creatine kinase-MB (CK-MB), prostacyclin (PGI_2) and tissues including glutathione (GSH). Also, the study of changes of histo-pathological parameters of the evaluated compounds compared to celecoxib as a reference standard was performed. All the obtained results were shown in **Table 4** and **Fig. 4.** The results revealed that celecoxib administration induced significant increase in the diagnostic biomarkers of myocardial damage [53–55] including Tn-I, LDH and CK-MB levels, as compared to normal control. Whereas, both **9b** and **9c** exhibited a significant lowering in these biochemical levels when compared to celecoxib treatment levels proofing their protective cardiovascular activity and much less risks. Moreover, serum TNF-α, a key player in the inflammatory response and cardiac depression [56], significantly increased after celecoxib treatment if compared to the control group, unlike groups that administered the newly synthesized compounds **9b** and **9c** that showed remarkably decrease in TNF-α concentration if compared to the celecoxib induced cardio-toxicity group.

Table 4: Results of serum TNF-α, Tn-I, LDH and CK-MB measurements in **9b**, **9c** and celecoxib.

Groups	**TNF-α** (pg/ml)	**Troponine-I** (pg/ml)	**LDH** IU/L	**CK-MB** IU/L
Normal control	78.67±3.75	74±4.61	1536±100	16±2.3
Celecoxib	748.67±43.15[a]	340±11.56[a]	2091.3±99.9[a]	95.33±4[a]
9b	322±11.9[b]	150±11.23[b]	1585±74.2[b]	22±4[b]
9c	265.67±7.3[ab]	108.67±2.60[b]	1473.3±28.57[b]	17±2.3[b]

Data analyzed by one-way ANOVA followed by Bonferroni test to enable comparing groups pairwise, (n = 6), [a]Significantly different from normal control group at $p < 0.05$. [b]Significantly different from celecoxib group at $p < 0.05$.

Tissue GSH, the important antioxidant in cardiac tissues, remarkably decreased in the celecoxib treated group confirming the previous studies which reported that celecoxib in chronic administration elevated the oxidative stress markers as lipid peroxidation and reduced GSH level through increasing

the oxidative damage of the kidney [57]. On the contrary, compounds **9b** and **9c** restored heart GSH level, where they significantly increased GSH levels compared to celecoxib group as shown in **Fig. 4.**

Meanwhile, PGI_2 plays an important role in cardiovascular health, [58] especially its ratio to thromboxane A_2 in blood, as the most potent endogenous inhibitor of platelet aggregation, where the decrease in PGI_2 levels indicates cardiomyopathy. In this regard, it was found that celecoxib and **9b** significantly decreased PGI_2 levels, if compared to normal control, while compound **9c** was not significantly different from the normal control. Furthermore, each of the tested compounds significantly increased PGI_2 level if compared to celecoxib, as shown in **Fig. 5**.

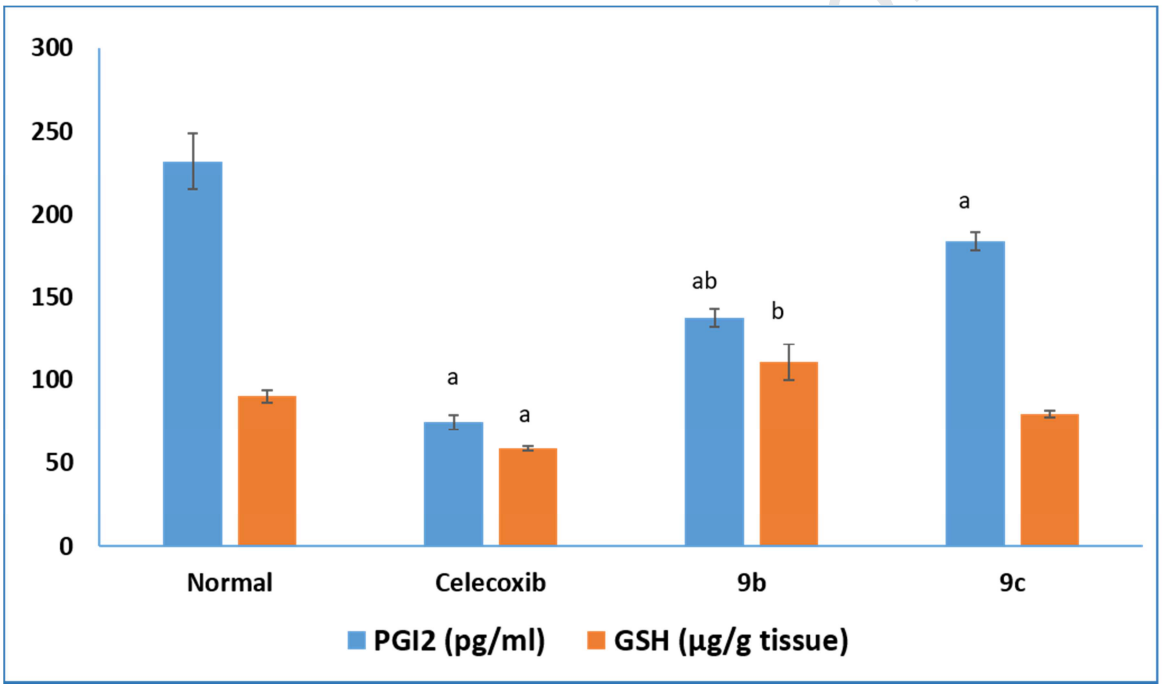

Fig. 5. Cardic glutathione (GSH) content and serum prostacyclin (PGI_2) level in different groups. Data analyzed by one-way ANOVA followed by Bonferroni test to compare groups pairwise, (n = 6). *[a]Significantly different from normal control group at p < 0.05. [b]Significantly different from celecoxib group at p < 0.05.*

Interestingly, histo-pathological studies revealed that the heart section obtained from rats exposed to celecoxib showed severe hemorrhage and edema between muscle bundles (B). While the heart sections obtained from rats exposed to **9b** (C) showed mild to moderate congestion and edema in myocardium blood vessels and in coronary artery. Also, the heart sections obtained from rats exposed

to **9c** (D) showed mild decongestant and mild edema on cardiac blood vessels and showed more or less normal muscle bundles, as shown in **Fig. 6**.

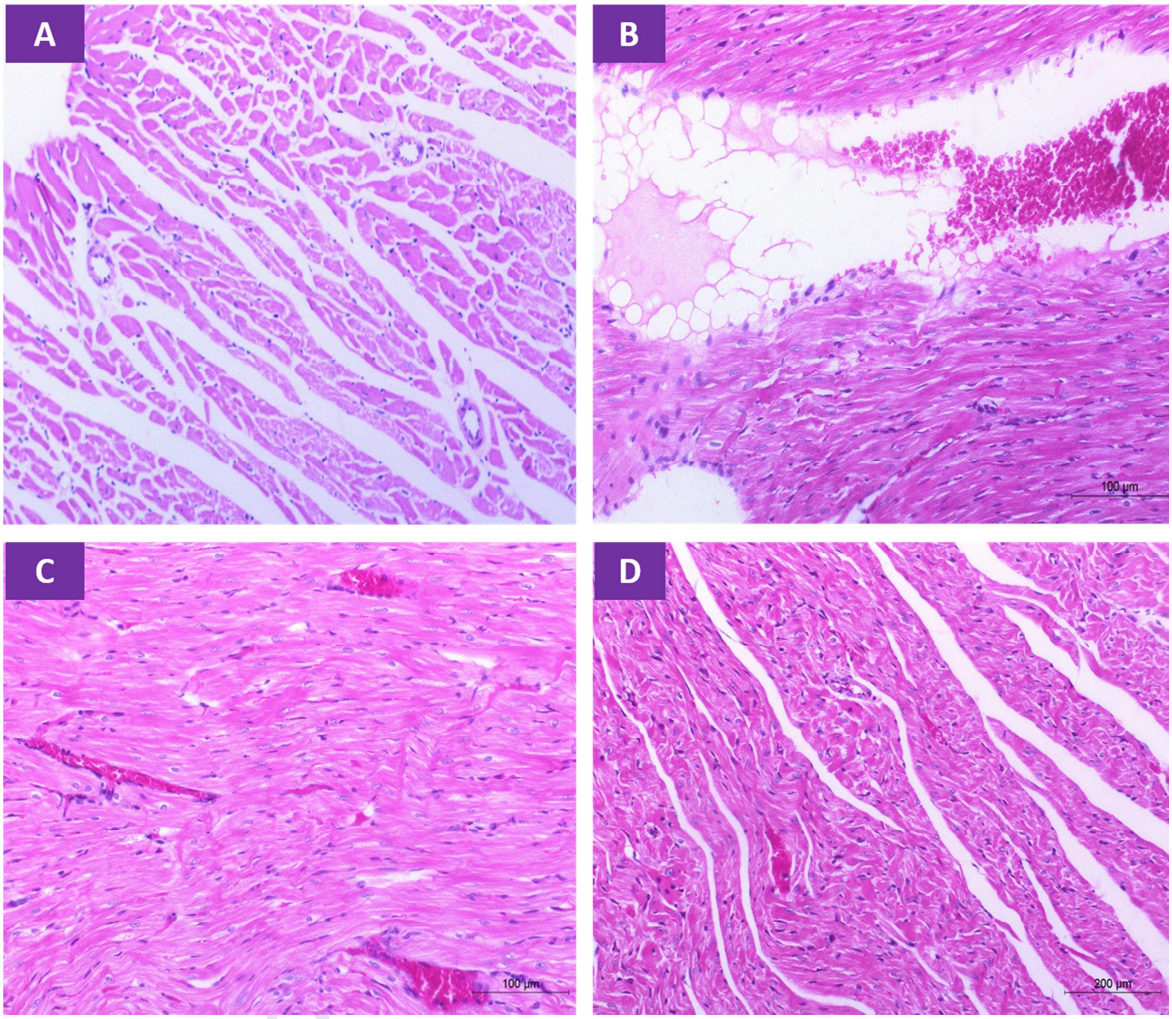

Fig. 6. Routine hematoxylin and eosin (H&E) stained sections of the left ventricle in animals' groups where (A) Control group; (B) Celecoxib administered group; (C) **9b** administered group; (d) **9c** administered group. (Routine hematoxylin and eosin (H&E) stained; 200x). Figure (A) shows normal myocardium. Figure (B) shows sever hemorrhage and edema between muscle bundles. Figures (C) and (D) show mild to moderate congestion and edema in the myocardium.

2.3. Molecular Docking:

The current study was accomplished to recognize the activity of the newly synthesized urea disubstituted-1,5-diarylpyrazole derivatives and know some structural perceptions into their binding manners and probable interactions with sEH enzyme. Accordingly, some active derivatives **(9a**, **9c**, **11a** and **11c)** in addition to some other inactive ones (**9e**, **9f** and **11e)**, for comparison, were docked into the active sites of sEH using LigandFit embedded in the Discovery Studio software (San Diego,

USA). The 3D crystal structure of sEH (PDB ID: 1VJ5) in complex with CIU781, respectively, were used for this docking simulation study [59,60]. The amino acid residues within a distance of 8 Å around the sEH co-crystallized ligands in the active pocket were isolated and the potential interactions and ligands orientation were inspected. The overlay of the top docking poses into sEH protein binding pocket was presented in **Fig. 7**, where the poses **9a**, **9c**, **11a**, **11c** and **AUDA** showed good shape complementarity with the active site of sEH enzyme.

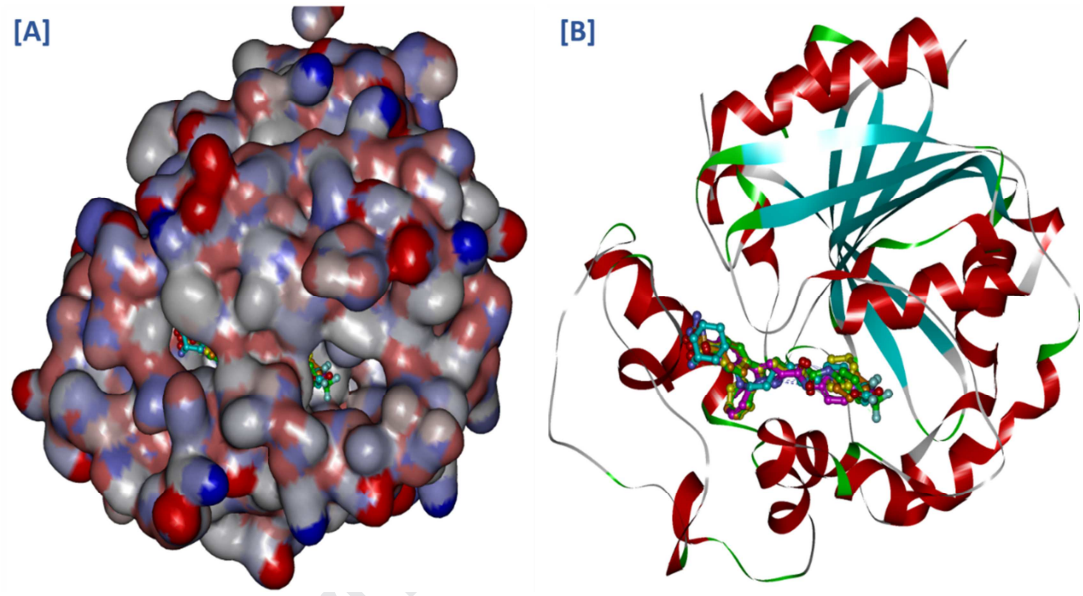

Fig. 7. Overlay of the top docked poses **9a**, **9c**, **11a**, **11c** and **AUDA** as a reference ligand into the sEH binding pocket (PDB code: 1VJ5); sEH protein is represented as: (A) Solid surface colored according to atom charges; (B) Secondary structure displayed in a flat ribbon style.

It was reported that the catalytic pocket of sEH consists of three main amino acids; Asp333, Tyr381, Tyr465, which are responsible for the activity of the enzyme [59–61]. Therefore, it always noticed that a network of hydrogen bonds formed between the urea or amide moieties in the potent sEH inhibitors and these important amino acids inside the hydrolase catalytic pocket. In doing so, the inspection of the docking results of the active derivatives **9a**, **9c** and **11c** showed that they all fit precisely inside the active site engaging some interactions including hydrogen bonds and π-π stacking. In general, it was found that the top docked poses adopted a common binding pattern and orientation where the phenyl-bearing sulfonamide moiety in the three compounds aligned towards His523, Trp524, Val415 and Leu416 amino acids residues while the phenyl-bearing trifluoromethyl

group was extended towards Trp334, Met337, Ilu373 and Phe379 residues forming some hydrophobic interactions, **Fig. 8(A-C)**. Their noticeable potency against sEH enzyme may greatly due to the obvious similarity between the binding patterns of these derivatives. It was conceptualized that the number and type of these interactions could explain the variation between these ligands in their potency. Compound **9c** was the most active derivative (IC_{50} = 0.4 nM) where it involved in the highest number and types of interactions. It formed five different H-bonds; one between the carbonyl oxygen of urea moiety and Try381, two between NH of urea and Asp333, one between the NH of the pyrazole ring and Try464 and the fifth between the NH_2 of the sulfonamide group and Leu416 residue. In addition, several π-π stacking between pyrazole ring and imidazole of His523 residue and two others between phenyl-bearing sulfonamide and the indole heterocycle of Trp524 amino acid, **Fig. 8(A)**. The decrease in the activity of **9a** (IC_{50} = 0.98 nM) compared with **9c** could be explained by the absence of some interactions such as H-bond with Leau416 and π-π stacking with Trp524 residue, **Fig. 8(B)**. However, the amide derivatives **11c** showed the least activity (IC_{50} = 1.2 nM) between the most active ones due to the sharp reduction in the number of interactions despite of adopting a similar orientation. The replacement of urea moiety with an amide one resulted in the absence of an important H-bond with Asp333 in the catalytic active site of sEH enzyme, **Fig. 8(C)**.

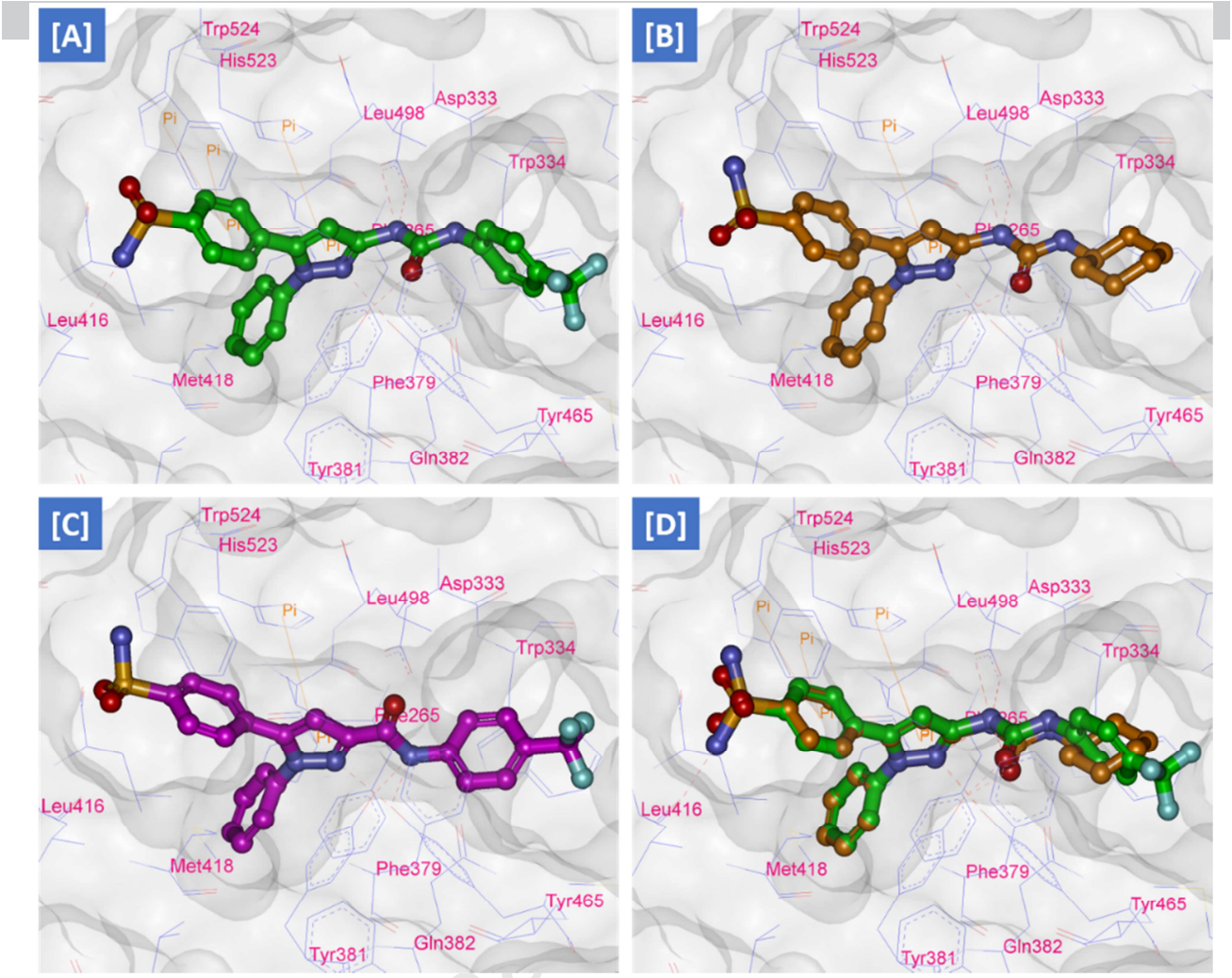

Fig. 8. (A) Docking and binding pattern of compound **9c** (green) into catalytic active pocket of sEH enzyme (PDB code: 1VJ5); (B) Docking and binding pattern of compound **9a** (orange) into catalytic active pocket of sEH enzyme; (C) Docking and binding pattern of compound **11c** (violet) into catalytic active pocket of sEH enzyme; (D) The superimposition of **9a** and **9c** docked poses within the catalytic active pocket of sEH enzyme. The poses were rendered as ball and stick model. π- π Interactions were represented as orange solid line. Hydrogen bonds were represented as dashed orange lines. All hydrogens were removed for the purposes of clarity.

Moreover, the analysis of the docking results of the inactive compounds **9f** and **11e** into the sEH active pocket specified that these two ligands shared a completely opposing orientation and dispositioning compared with the previously docked active derivatives **(9a**, **9c**, **11a** and **11c), Fig. 9 (A and B)**. It was found that the phenyl-bearing sulfonamide core was located near Trp334, Met337, Ilu373 and Phe379 residues causing some bulkiness reflected in the sharp decrease in activity as in compound **9f** which showed the least potency (IC_{50} = 4.01 nM). While, the phenyl-bearing

trifluoromethyl directed towards His523, Trp524, Val415 and Leu416 amino acids residues, **Fig. 9(A)**. Moreover, amide derivative **11e** adopted a similar orientation to that of **9f** with a slight increase in activity (IC_{50} = 3.31 nM) noticed with increasing the carbon side chain length, **Fig. 9(B)**. The docking study was compatible with the *in vitro* assay results, proving that hybridization between the urea or amide sEH pharmacophoric moiety and the sulfonamide-bearing diarylpyrazole COX-2 core are good leads for further optimization.

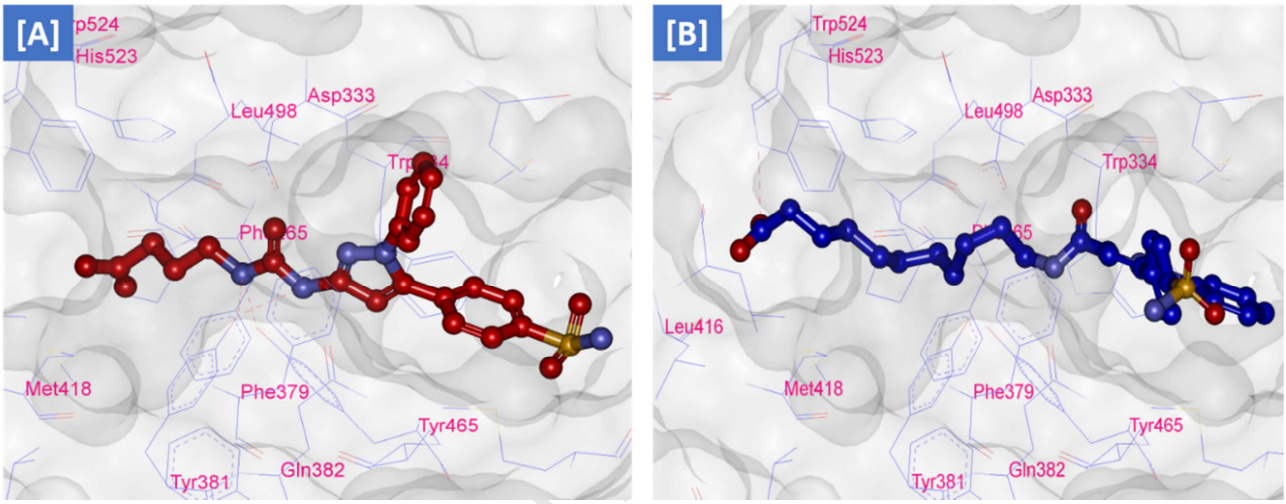

Fig. 9. (A) Docking and binding pattern of compound **9f** (magenta red) into the catalytic active pocket of sEH enzyme (PDB code: 1VJ5); (B) Docking and binding pattern of compound **11e** (blue) catalytic active pocket of sEH enzyme. The poses were rendered as ball and stick model. All hydrogens were removed for the purposes of clarity.

2.4. Physicochemical parameters:

According to the great effect of physicochemical properties of any compound on its bioavailability and its possible druggability, computational prediction of the physicochemical properties of the synthesized compounds has been performed on the basis of Lipinski's rule of five (RO5) [62]. The chemo-informatic properties of the synthesized compounds were predicted using Molinspiration tool [63,64] and outlined in **Table 5**. All synthesized compounds exhibited good oral bioavailability because all of them showed no or only one violation from Lipinski's rule except two compounds **9e** and **11f**. Moreover, calculated absorption (%ABS) complied the ability of the compounds to elicit promising pharmacokinetic properties, where %ABS is ranging from 55-72%.

Table 5. Calculated absorption, polar surface area and Lipinski parameters of the target compounds **9a-f** and **11a-f**.

Compound	%ABS[a]	tPSA[b]	Nrotb[c]	nON ≤10[d]	nOHNH ≤5[e]	miLog*P* ≤5	MW ≤500	n violations ≤1
9a	67.9	119.12	5	8	4	3.56	439.54	0
9b	67.9	119.12	5	8	4	4.58	491.62	0
9c	67.9	119.12	6	8	4	4.25	501.49	1
9d	61.86	136.63	7	10	3	2.92	497.58	0
9e	55.04	156.41	15	10	5	4.98	541.67	3
9f	55.04	156.41	8	10	5	1.45	443.49	1
11a	72.06	107.09	5	7	3	3.37	424.53	0
11b	72.06	107.09	5	7	3	4.38	476.6	0
11c	72.06	107.09	6	7	3	4.05	486.48	0
11d	66.01	124.61	7	9	2	2.72	482.56	0
11e	59.19	144.39	15	9	4	4.78	526.66	3
11f	59.19	144.39	8	9	4	1.25	428.47	1

[a]% ABS: Calculated absorption; [b]tPSA: Topological polar surface area; [c]nrotb: Number of rotatable bonds; [d]nON≤10: Number of hydrogen bond acceptors less than or equal to 10 and [e]nOHNH≤5: Number of hydrogen bond donors less than or equal to 5.

3. Conclusion:

Novel series of 1,5- diarylpyrazole series of urea linked (**9a-f**) and amide linked (**11a-f)** compounds were designed, synthesized and evaluated as dual inhibitors of both COX-2/sEH enzymes in an attempt to preserve the preferred pharmacological activity of the selective COX-2 inhibitors with avoiding their serious associated cardiovascular side effects through sEH inhibition. The *in vivo* and *in vitro* biological results revealed that compound **9c**, which possessed *p*-triflouromethyl anilinyl moiety directly attached to a urea linker, was the most potent dual COX-2/sEH inhibitor (COX-2 IC_{50} = 1.24 μM; *SI* = 7.03; sEH IC_{50} = 0.40 nM) and showed the highest *in vivo* activities as analgesic (65.67% writhing inhibition) and anti-inflammatory (98.15% edema inhibition) agent, followed by compound **9b**, which elicited good COX-2/sEH inhibition (COX-2 IC_{50} = 1.85 μM; *SI* = 6.41; sEH IC_{50} = 0.55

nM) and high anti-inflammatory activity (93.79% Edema inhibition). Regarding the cardiovascular system evaluation, the results were consistent with both *in vivo* and *in vitro* inhibitory activities values that affirmed the good activities of compound **9c** affording a perfect cardio-protection and less cardiovascular liabilities, in contrast to the selective COX-2-induced cardiotoxicity. This was proved via decreasing the cardiac diagnostic biomarkers of myocardial damage including Tn-I, LDH and CK-MB level, consort with increasing in the antioxidant biomarker GSH, and the anti-platelets aggregation agent PGI_2 levels. The aforementioned results revealed that compound **9c,** named 4-(1-phenyl-3-(3-(4-(trifluoromethyl)phenyl)ureido)-1H-pyrazol-5-yl)benzenesulfonamide (PTPUP), could be considered as a promising candidate with potent dual COX-2/sEH inhibitory activities to be further developed as a safe anti-inflammatory/analgesic lead attending with significant less cardiovascular risks than current selective COX-2 drugs.

4. Experimental protocols:

4.1. Chemistry:

All chemical reagents and solvents were procured from commercial suppliers and were utilized with no further purification. Melting points were uncorrected and were implemented by open capillary tube methods using IA 9100MK-Digital melting point apparatus. Elemental analysis was performed at the micro-analytical center at the regional center for mycology and biotechnology, Al-Azhar University. Infrared spectra were reported on Bruker FT-IR spectrophotometer Vector 22 and recorded in wave number (cm^{-1}) using KBr discs at the micro-analytical center, Faculty of Science, Cairo University. ^{1}H NMR and ^{13}C NMR spectra were executed with Bruker APX400 spectrometer at 400 MHz and 101 MHz, respectively in the specified solvent at the Faculty of Pharmacy, Beni-Suef University. The chemical shifts were outlined on the δ scale and *J* values were recorded in Hz. Mass spectra were reported on Finnegan MAT, SSQ 7000, Mass spectrometer, at 70 eV (EI) at the micro-analytical center, Faculty of Science, Cairo University. Thin layer chromatography (TLC) was carried out using Macherey-Nagel Alugram Sil G/UV254 silica gel plats and Petroleum ether-ethyl acetate (6:4) as the eluting system.

1-phenyl-5-(4-sulfamoylphenyl)-1H-pyrazole-3-carbonyl azide **7**. A solution of $NaNO_2$ (0.87 g, 1.0 mmol) in cold water (3 mL) was added to a cold solution (0-5 ^oC) of hydrazide **6** (0.357 g, 1.0 mmol) in acetic acid (6 mL), 1N HCl (3 ml), and water (25 mL). The reaction mixture was allowed to be stirred at 0-5 °C for 15 min followed by extraction with ethyl acetate (30 mL) producing yellow syrup. The formed yellow syrup was washed with cold 3% $NaHCO_3$, H_2O, dried over anhydrous Na_2SO_4 and used in the next step without purification.

General procedure A for synthesis of compounds (9a-9f): The acyl azide **7** (0.78 g, 2.14 mmol) was dissolved in anhydrous toluene (5 mL) and the mixture was exposed to heating under reflux for 1 hour under N_2. After completion of the reaction, the reaction mixture was allowed to cool to room temperature followed by addition of the appropriate amine (2 mmol) in the presence of pyridine. The mixture was heated under reflux for 24 hours subsequently pouring onto ice/H_2O containing few drops of conc HCl. The compound was extracted with ethyl acetate, drying over anhydrous magnesium sulfate followed by purification of the resulted residue by column chromatography using petroleum ether to ethyl acetate gradient to elute the final compounds **9a-9f** in good yields.

4-(3-(3-cyclohexylureido)-1-phenyl-1H-pyrazol-5-yl)benzenesulfonamide **9a**. General procedure A, as white solid (54%); m.p. 215°C. IR (cm^{-1}): 3415 (NH), 3100 (CH aromatic), 2929 (CH aliphatic), 1660 (NHCONH), 1510 (C=N), 1339, 1161 (SO_2NH_2). ^1H NMR (400 MHz, DMSO-d_6): δ 9.00 (s, 1H, NH exchangeable with D_2O), 7.77-7.79 (d, J = 8 Hz, 2H, Ar-H), 7.41-7.43 (m, 5H, 3 H of Ar-H and 2H of SO_2NH_2 exchangeable with D_2O), 7.35-7.37 (m, 2H, Ar-H), 7.27-7.29 (m, 2H, Ar-H), 6.69 (s, 1H, NH exchangeable with D_2O), 6.59 (s, 1H, Pyrazolyl-H), 3.55 (m, 1H, -NHCHCH$_2$-), 1.81-1.83 (m, 2H, -CHCH(H)CH$_2$-), 1.61-1.70 (m, 2H, -CHCH(H)CH$_2$-), 1.51-1.55 (m, 2H, -(CH$_2$)$_2$CH$_2$(CH$_2$)$_2$-), 1.17-1.35 (m, 4H, -CH$_2$CH$_2$CH$_2$CH-). ^{13}C NMR (101MHz, DMSO-d_6): δ 160.5, 148.2, 145.2, 144.9, 143.9, 142.0, 131.9, 129.5, 129.0, 126.1, 125.5, 108.8, 48.2, 32.8, 25.6, 25.4. MS (EI): *m/z* 439 (M^+). Anal. Calcd. For $C_{22}H_{25}N_5O_3S$: C, 60.12; H, 5.73; N, 15.93. Found: C, 59.95; H, 5.88; N, 16.12.

4-(3-(3-adamantylureido)-1-phenyl-1H-pyrazol-5-yl) benzenesulfonamide **9b**. General procedure A, white solid (53%); m.p. 265°C. IR (cm^{-1}): 3387 (NH), 3278 (CH aromatic), 2904 (CH aliphatic), 1678 (NHCONH), 1339, 1161 (SO_2NH_2), 1508 (C=N).^{1}H NMR (400 MHz, DMSO-d_6): δ 8.88 (s, 1H, NH exchangeable with D_2O), 7.77-7.79 (d, *J* = 8 Hz, 2H, Ar-H), 7.69-7.72 (s broad, 1H, NH exchangeable with D_2O), 7.41-7.43 (m, 5H, 3 H of Ar-H and 2H of SO_2NH_2 exchangeable with D_2O), 7.33-7.36 (m, 2H, Ar-H), 7.27-7.29 (m, 2H, Ar-H), 6.58 (s, 1H, Pyrazolyl-H), 2.02-2.05 (m, 3H, -$(CH_2)_2$CH$(CH_2)_2$-), 1.90-1.89 (m, 6H, -NHCCH_2-), 1.65-1.59 (m, 6H, -CHCH_2CH-). ^{13}C NMR (101MHz, DMSO-d_6): δ 153.5, 143.4, 142.4, 142.2, 130.3, 129.3, 128.9, 127.2, 127.1, 124.6, 119.6, 99.9, 50.4, 42.1, 36.5, 29.4. MS (EI): *m/z* 491 (M^+). Anal. Calcd. For $C_{26}H_{29}N_5O_3S$: C, 63.52; H, 5.95; N, 14.25. Found: C, 63.81; H, 6.08; N, 14.37.

4-(1-phenyl-3-(3-(4-(trifluoromethyl)phenyl)ureido)-1H-pyrazol-5-yl)benzenesulfonamide **9c**.General procedure A, yellow solid (63%); m.p. 278°C. IR (cm^{-1}): 3371 (NH), 3167 (CH aromatic), 1689 (NHCONH), 1330, 1161 (SO_2NH_2), 1508. (C=N). ^{1}H NMR (400 MHz, DMSO-d_6): δ 10.13 (s, 1H, NH exchangeable with D_2O), 9.77 (s, 1H, NH exchangeable with D_2O), 7.88-7.90 (d, *J* = 8 Hz, 2H, Ar-H), 7.59-7.61 (d, *J* = 8 Hz, 2H, Ar-H), 7.51-7.54 (m, 3H, Ar-H), 7.43-7.44 (m, 4H, 2H of Ar-H and 2H of SO_2NH_2 exchangeable with D_2O), 7.34-7.36 (m, 2H, Ar-H), 7.18 (s, 1H, Pyrazolyl-H), 7.16-7.17 (m, 2H, Ar-H) . ^{13}C NMR (101MHz, DMSO-d_6): δ 159.9, 144.3, 144.1, 144.0, 130.8, 129.9, 129.5, 129.3, 129.3, 127.4, 126.6, 126.4, 126.4, 126.2, 125.9, 120.7, 109.1. MS (EI): *m/z* 501 (M^+). Anal. Calcd. For $C_{23}H_{18}F_3N_5O_3S$: C, 55.09; H, 3.62; N, 13.97. Found: C, 55.24; H, 3.81; N, 14.15.

Ethyl 1-((1-phenyl-5-(4-sulfamoylphenyl)-1H-pyrazol-3-yl)carbamoyl)piperidine-4-carboxylate **9d**. General procedure A, buff solid (57%); m.p. 189 °C. IR (cm^{-1}): 3414 (NH), 3100 (CH aromatic), 2930 (CH aliphatic), 1720 (COOCH_2CH_3), 1630 (NHCONH), 1508 (C=N), 1338, 1161 (SO_2NH_2). ^{1}H NMR (400 MHz, DMSO-d_6): δ 9.42 (s, 1H, NH exchangeable with D_2O), 7.77-7.79 (d, *J* = 8 Hz, 2H, Ar-H), 7.41-7.43 (m, 5H, 3 H of Ar-H and 2H of SO_2NH_2 exchangeable with D_2O), 7.35-7.37 (m, 2H, Ar-H), 7.27-7.29 (m, 2H, Ar-H), 6.59 (s, 1H, Pyrazolyl-H), 4.03-4.09 (m, 4H, 2H of CH_2CH_3

and 2H of -NCH(H)CH_2-), 2.93 (m, 1H, -NCH(H)CH_2-), 2.60 (m, 1H, -NCH(H)CH_2-), 2.25 (m, 1H, -CH_2CHCO-), 1.77-1.92 (m, 2H, -CHC$H_2$$CH_2$-), 1.51-1.56 (m, 2H,-CHC$H_2$$CH_2$-), 1.17-1.20 (t, *J* = 6 Hz, 3H, -CH_2CH_3-). ^{13}C NMR (101MHz, DMSO-d_6): δ 174.4, 161.7, 148.3, 144.0, 143.7, 142.0, 129.5, 129.3, 129.3, 129.2, 127.2, 126.0, 110.4, 60.5, 48.2, 29.1, 28.2, 14.6. MS (EI): *m/z* 497 (M^+). Anal. Calcd. For $C_{16}H_{15}N_5O_3S$: C, 58.69; H, 5.71; N, 13.69. Found: C, 58.90; H, 5.73; N, 13.84.

11-(3-(1-phenyl-5-(4-sulfamoylphenyl)-1H-pyrazol-3-yl)ureido)undecanoic acid **9e**. General procedure A, white solid (63%); m.p. 245 °C. IR (cm^{-1}): 3400-2500 (COOH), 3035 (CH aromatic), 2970 (CH aliphatic), 1697 (C=O), 1630 (C=O), 1504 (C=N), 1334, 1161 (SO_2NH_2). ^{1}H NMR (400 MHz, DMSO-d_6): δ 9.08 (s, 1H, NH exchangeable with D_2O), 7.77-7.79 (d, *J* = 8 Hz, 2H, Ar-H), 7.41-7.43 (m, 5H, 3 H of Ar-H and 2H of SO_2NH_2 exchangeable with D_2O), 7.36-7.38 (m, 2H, Ar-H), 7.27-7.29 (m, 2H, Ar-H), 6.66 (s, 1H, NH exchangeable with D_2O), 6.59 (s, 1H, Pyrazolyl-H), 3.09-3.14 (m, 2H,-NHC$H_2$$CH_2$-), 2.16-2.19 (m, 2H,-$CH_2CH_2$COOH), 1.44-1.50 (m, 4H, 2H of -CH_2C$H_2$$CH_2$COOH and 2H of –NHC$H_2CH_2$$CH_2$-), 1.26-1.28 (m, 12H, -$CH_2CH_2$$CH_2$-). ^{13}C NMR (101MHz, DMSO-d_6): δ 175.1, 163.2, 154.9, 150.8, 143.6, 142.4, 142.3, 130.3, 129.3, 128.9, 127.0, 124.7, 99.9, 34.2, 30.1, 29.4, 29.3, 29.2, 29.0, 26.8, 25.0. MS (EI): *m/z* 541 (M^+). Anal. Calcd. For $C_{27}H_{35}N_5O_5S$: C, 59.87; H, 6.51; N, 12.93. Found: C, 60.04; H, 6.61; N, 13.19.

4-(3-(1-phenyl-5-(4-sulfamoylphenyl)-1H-pyrazol-3-yl)ureido)butanoic acid **9f**. General procedure A, white solid (51%); m.p. 245 °C. IR (cm^{-1}): 3500-2800 (COOH), 3367 (NH), 3070 (CH aromatic), 2929 (CH aliphatic), 1693 (COOH), 1589 (NHCONH), 1512 (C=N), 1334, 1161 (SO_2NH_2). ^{1}H NMR (400 MHz, DMSO-d_6)**:** δ 10.12 (s, 1H, COOH exchangeable with D_2O), 9.75 (s, 1H, NH exchangeable with D_2O), 7.88-7.90 (d, *J* = 8 Hz, 2H, Ar-H), 7.59-7.61 (d, *J* = 8 Hz, 2H, Ar-H), 7.50-7.52 (m, 2H, Ar-H), 7.43-7.44 (m, 3H, 1H of Ar-H and 2H of SO_2NH_2 exchangeable with D_2O), 7.34-7.36 (m, 2H, Ar-H), 7.18 (s, 1H, Pyrazolyl-H), 7.16 (s, 1H, NH exchangeable with D_2O), 3.17 (m, 2H, -NHC$H_2$$CH_2$), 2.27 (m, 2H, -$CH_2CH_2$COOH), 1.24 (m, 2H, -$CH_2CH_2$$CH_2$-). ^{13}C NMR (101MHz, DMSO-d_6): δ 208.0, 154.4, 154.2, 149.5, 143.6, 142.6, 142.3, 130.2, 129.3, 129.3, 127.1,

125.1, 100.5, 61.0, 28.5, 14.9. MS (EI): *m/z* 443 (M^+). Anal. Calcd. For $C_{20}H_{21}N_5O_5S$: C, 54.17; H, 4.77; N, 15.79. Found: C, 54.37; H, 4.89; N, 16.01.

General procedure B for preparation of compounds 11a-11f: A solution of ester **5** (0.37g, 1 mmol) in methanol was treated with KOH (0.11 g, 2 mmol) and heated under reflux for 12 hours. The mixture was acidified with 1N HCl after cooling to room temperature. The solvent was then evaporated to give buff solid that recrystallized from methanol to furnish the desired compound (0.33g, 97% yield) as reported [48]. To a suspension of acid (0.342 g, 1mmol) in CH_2Cl_2, 2 mL of $SOCl_2$ was added and heated under reflux for 3 hours. Evaporation the solvent was carried out under vacuum to give a residue of the corresponding acyl chloride that utilized in the following step without purification. To a solution of acyl chloride in CH_2Cl_2, few drops of trimethylamine were added followed by appropriate amine (1 mmol) and was left under stirring at room temperature overnight. The solvent was evaporated, washing the residue with water, extraction with ethyl acetate followed by drying on anhydrous $MgSO_4$. Purification of the obtained residue was carried out by column chromatography technique using hexane and ethyl acetate (8:2) to afford the final compounds **11a-11f** in good yields.

to afford the titled compound.

N-cyclohexyl-1-phenyl-5-(4-sulfamoylphenyl)-1H-pyrazole-3-carboxamide **11a**. General procedure B, white solid (85%); m.p. 240 °C. IR (cm^{-1}): 3390 (NH), 3132 (CH aromatic), 2931 (CH aliphatic), 1643 (CONH), 1323, 1161 (SO_2NH_2), 1550 (C=N). ^{1}H NMR (400 MHz, DMSO-d_6): δ 8.06-8.08 (m, 1H, Ar-H), 7.86-7.88 (d, *J* = 8 Hz, 2H, Ar-H), 7.51-7.57 (m, 4H, 2H of Ar-H and 2H of SO_2NH_2 exchangeable with D_2O), 7.41 (m, 3H, 2H of Ar-H and 1H of NH exchangeable with D_2O), 7.30-7.31 (m, 2H, Ar-H), 7.04 (s, 1H, Pyrazolyl-H), 3.78 (m, 1H, -NHCHCH$_2$-), 1.72-1.82 (m, 4H, -NHCH(CH$_2$)$_2$CH$_2$-), 1.61-1.63 (m, 2H, -(CH$_2$)$_2$CH$_2$(CH$_2$)$_2$-), 1.29-1.39 (m, 4H, -CHCH$_2$CH$_2$CH$_2$-). ^{13}C NMR (101MHz, DMSO-d_6): δ 160.6, 148.5, 144.9, 143.9, 142.1, 129.6, 129.4, 129.30 129.2,

127.1, 126.3, 108.8, 48.2, 32.8, 25.6, 25.4. MS (EI): *m/z* 424 (M^+). Anal. Calcd. For $C_{22}H_{24}N_4O_3S$ C, 62.24 H, 5.70; N, 13.20. Found: C, 62.39; H, 5.83; N, 13.13.

N-adamantyl-1-phenyl-5-(4-sulfamoylphenyl)-1H-pyrazole-3-carboxamide **11b**. General procedure B, white solid (45%); m.p. 198 °C. IR (cm^{-1}): 3305 (NH), 3070 (CH aromatic), 2908 (CH aliphatic), 1666 (CONH), 1334, 1161 (SO_2NH_2), 1504 (C=N). ^{1}H NMR (400 MHz, DMSO-d_6): δ 7.88-7.90 (d, *J* = 8 Hz, 2H, Ar-H), 7.55-7.62 (m, 3H, 2H of Ar-H and 1H of NH exchangeable with D_2O), 7.52 (s, 2H, SO_2NH_2 exchangeable with D_2O), 7.40-7.41 (m, 3H, Ar-H), 7.30-7.31 (m, 2H, Ar-H), 7.09 (s, 1H, Pyrazolyl-H), 1.92-2.01 (m, 6H, -NHCCH_2-), 1.82 (m, 6H, -CHCH_2CH-), 1.71 (m, broad 2H, -CH_2CHCH_2-), 1.57-1.60 (m, 1H, -CH_2CHCH_2-). ^{13}C NMR (101MHz, DMSO-d_6): δ 160.6, 148.2, 145.2, 143.9, 142.0, 129.5, 129.3, 129.2, 127.2, 126.2, 125.9, 108.8, 53.5, 37.2, 31.9, 27.2. MS (EI): *m/z* 476 (M^+). Anal. Calcd. For $C_{26}H_{28}N_4O_3S$ C, 65.52 H, 5.92; N, 11.76. Found: C, 65.80; H, 6.07; N, 11.89.

1-phenyl-5-(4-sulfamoylphenyl)-N-(4-(trifluoromethyl)phenyl)-1H-pyrazole-3-carboxamide **11c**. General procedure B, yellow solid (65%); m.p. 125 °C. IR (cm^{-1}): 3302 (NH), 3070 (CH aromatic), 1666 (CONH), 1504 (C=N), 1334, 1161 (SO_2NH_2). ^{1}H NMR (400 MHz, DMSO-d_6): δ 10.61 (s, 1H, 1NH exchangeable with D_2O), 8.10-8.08 (d, *J* = 8 Hz, 2H, Ar-H), 7.91-7.89 (d, *J* = 8 Hz, 2H, Ar-H), 7.75-7.72 (d, *J* = 8 Hz, 2H, Ar-H), 7.61-7.63 (d, *J* = 8 Hz, 2H, Ar-H), 7.52 (m, 2H, SO_2NH_2 exchangeable with D_2O), 7.43-7.44 (m, 3H, Ar-H), 7.35-7.36 (m, 2H, Ar-H), 7.24 (s, 1H, Pyrazolyl-H). ^{13}C NMR (101MHz, DMSO-d_6): δ 160.5, 147.8, 145.4, 145.1, 144.3, 142.7, 141.9, 129.6, 129.3, 129.3, 129.2, 127.2, 126.6, 126.4, 126.3, 120.4, 109.4. MS (EI): *m/z* 486 (M^+). Anal. Calcd. For $C_{23}H_{17}F_3N_4O_3S$ C, 56.79 H, 3.52; N, 11.52. Found: C, 56.96; H, 3.71; N, 11.80.

Ethyl 1-(1-phenyl-5-(4-sulfamoylphenyl)-1H-pyrazole-3-carbonyl)piperidine-4-carboxylate **11d**. General procedure B, yellowish brown solid (67%); m.p. 256 °C. IR (cm^{-1}): 3464 (NH_2 of SO_2NH_2), 3062 (CH aromatic), 2929 (CH aliphatic), 1708 (COOCH_2CH_3), 1597 (CON), 1489 (C=N), 1354, 1168 (SO_2NH_2). ^{1}H NMR (400 MHz, DMSO-d_6): δ 7.88-7.90 (d, *J* = 8 Hz, 2H, Ar-H), 7.51-7.53 (m,

3H, Ar-H), 7.41(m, 4H, 2H of SO_2NH_2 exchangeable with D_2O and 2H of Ar-H), 7.32 (m, 2H, Ar-H), 6.94 (s, 1H, Pyrazolyl-H), 4.39-4.45 (m, 2H, CH_2CH_3), 4.03-4.09 (m, 4H, -NCH_2CH_2-), 3.27-3.37 (m, 1H, -CH_2CHCO-), 2.93-2.99 (m, 2H, -$CHCH_2CH_2$-), 2.60-2.69 (m, 2H, -$CHCH_2CH_2$-), 2.44-2.51 (m, 3H, -CH_2CH_3-). ^{13}C NMR (101MHz, DMSO-d_6): δ 174.3, 161.9, 148.3, 144.0, 143.7, 142.0, 129.5, 129.4, 129.3, 129.2, 127.2, 126.0, 110.4, 60.5, 46.2, 28.2, 28.1, 14.5. MS (EI): *m/z* 482 (M^+). Anal. Calcd. For $C_{24}H_{26}N_4O_3S$ C, 59.74 H, 5.43; N, 11.61 Found: C, 59.92; H, 5.67; N, 11.83.

11-(1-phenyl-5-(4-sulfamoylphenyl)-1H-pyrazole-3-carboxamido)undecanoic acid **11e**. General procedure B, yellow solid (67%); mp 158 °C. IR (cm^{-1}): 3400-2650 (OH of acid), 3379 (NH), 3259 (CH aromatic), 2924 (CH aliphatic), 1708 (COOH), 1651(CONH), 1338, 1161 (SO_2NH_2), 1566 (C=N). ^{1}H NMR (400 MHz, DMSO-d_6): δ 8.33 (s, 1H, NH exchangeable with D_2O), 7.85-7.87 (d, *J* = 8 Hz, 2H, Ar-H), 7.49-7.54 (m, 4H, 2H of Ar-H and 2H of SO_2NH_2 exchangeable with D_2O), 7.42-7.40 (m, 3H, Ar-H), 7.29-7.32 (m, 2H, Ar-H), 7.02 (s, 1H, Pyrazolyl-H), 3.23-3.28 (m, 2H, -$NHCH_2CH_2$-), 2.16-2.19 (m, 2H,-CH_2CH_2COOH), 1.44-150 (m, 4H, 2H of -$CH_2CH_2CH_2COOH$ and 2H of -$NHCH_2CH_2CH_2$-), 1.24-1.39 (m, 12H, -$CH_2CH_2CH_2$-). ^{13}C NMR (101MHz, DMSO-d_6): δ 175.1, 161.2, 148.4, 144.9, 143.9, 142.1, 129.6, 129.5, 129.3, 129.2, 127.1, 126.2, 108.7, 34.3, 29.7, 29.4, 29.4, 29.2, 29.0, 26.9, 25.0. MS (EI): *m/z* 526 (M^{+1}). Anal. Calcd. For $C_{27}H_{34}N_4O_5S$: C, 61.58; H, 6.51; N, 10.64. Found: C, 61.89; H, 6.73; N, 10.41.

4-(1-phenyl-5-(4-sulfamoylphenyl)-1H-pyrazole-3-carboxamido)butanoic acid **11f**. General procedure B, white solid (60%). m.p. 156 °C. IR (cm^{-1}): 3421-2931 (OH of acid), 3332 (NH), 3182 (CH aromatic), 2931 (CH aliphatic), 1678 (COOH), 1589 (CONH), 1512 (C=N), 1338, 1161 (SO_2NH_2). ^{1}H NMR (400 MHz, DMSO-d_6): δ 10.27 (s, 1H, COOH exchangeable with D_2O), 7.80-7.82 (d, *J* = 8 Hz, 2H, Ar-H), 7.45 (d, *J* = 8 Hz, 2H, SO_2NH_2 exchangeable with D_2O), 7.38-7.41 (m, 5H, Ar-H), 7.29-7.30 (m, 2H, Ar-H), 6.76 (s, 1H, Pyrazolyl-H), 4.13-4.18 (m, 2H, -$NHCH_2$-), 3.60-3.63 (m, 1H, -CH(H)COOH-), 2.34-2.37 (m, 1H, -CH(H)COOH-), 1.43 (s, 1H, NH exchangeable with D_2O), 1.23-1.25 (m, 2H,-$CH_2CH_2CH_2$-). ^{13}C NMR (101MHz, DMSO-d_6): δ 174.7, 159.1, 157.2, 155.2, 145.1, 140.2, 131.1, 129.4, 129.3, 127.6, 126.7, 120.8, 115.7, 31.6, 25.0, 21.5. MS (EI): *m/z*

428 (M^+). Anal. Calcd. For $C_{20}H_{20}N_4O_5S$ C, 56.06 H, 4.70; N, 13.08. Found: C, 56.34; H, 4.87; N, 13.29.

4.2. Biological screening:

4.2.1. *In vitro* Assay:

4.2.1.1. COXs inhibitory assay:

The inhibitory activity of the tested compounds against both COX-1 and COX-2 enzymes was monitored using enzyme immunoassay (EIA) kits from Cayman Chemical Company (catalogue number 701070 and 701080, Ann Arbor, MI) according manufacturer's directions and as referenced previously [65,66]. The assay depends on measuring the concentration of $PGF_{2\alpha}$, produced from PGH_2, via reduction with stannous chloride, through enzyme immunoassay (acetylcholine esterase competitive EIA) via a broadly specific antiserum that linked to all the major PG compounds. The yellow color, produced as a result of the reaction of bounded reagent with Ellman's reagent (contain acetylcholine esterase substrate) after removal of unbounded reagent, was determined spectrophotometrically at λ = 412 nm. Substantially, to the mixture of 960 µL of buffer solution (0.1 M Tris pH 8.0 containing 5 mM EDTA and 2 mM phenol) and COX-1/2 (10 µL) enzyme in presence of heme (10 µL), a volume of 20 µL of compounds (final conc of 1 µM) was added. The enzymes were pre-incubated with the tested compounds for 5 min at 37 °C before addition of 10 µL arachidonic acid (100 mM). After 2 min, termination of the COX reaction was carried out using 50 µL of 1M HCl. The inhibitory activity and IC_{50} were determined by performing the comparison between the tested compounds and the various control incubations.

4.2.1.2. In vitro sEH IC_{50} assay:

IC_{50} values were determined using a cell-based assay system of 96-well format (41). Epoxy Flour 7, a sensitive fluorescent substrate, was utilized to monitor the activity of the enzyme through its hydrolysis by sEH to the fluorescent 6-methoxy-2-naphthaldehyde that could be monitored (λ_{em} = 330 nm, λ_{ex} = 465 nm). Briefly, the assay was carried out through incubation of 10 µl of compounds

buffer or 10 µl of the AUDA solution to appropriate wells. For positive control wells, 100 µl of the 10 ng/ml sEH positive control (substrate) was prepared to two wells. Then, 200 µl of 6-methoxy-2-Naphthaldehyde was added. Standards were prepared above to corresponding wells of the black plate. 100 µl of the substrate solution was added to each well, except the standards, and the plate was allowed to incubate at 37 °C for 30 minutes. The fluorescent intensity of each well (excitation = 330 nm; emission = 465 nm) was read.

4.2.2. *In vivo* Assays:

4.2.2.1. Analgesic screening:

Acetic-acid induced writhing method in mice was supervened for evaluation of the analgesic activity of compounds **9a-f**, **11a-f,** as performed by *koster et al* [49]. The randomly selected albino mice of either sex (20-30g), were gained from animal house, Nahda University, Beni-Suef, and were subsequently distributed into 15 groups, 4 mice each. One group was left as a control, while the other group's animals orally administered 10mg/kg of the tested compounds and celecoxib, one hour before induction of pain through intra-peritoneal injection of 0.01mL/g of 0.6%v/v acetic acid. Observing the animals was carried out after 5 min of induction of pain. Recording and counting the writhing episodes including arching the back, protraction of body and stretching of hind limbs for 20 minutes was recorded.

4.2.2.2. Anti-inflammatory screening:

Evaluation of the anti-inflammatory activity of the tested compounds was carried out using carrageenan-induced paw edema model that was defined by Winter *et al.* was used to evaluate [50]. The experiments were performed on albino rats of either sex weighing 120-150 g, obtained from animal house, Nahda University, Beni-Suef. Rats were divided into groups of four animals after housing in a stainless-steel cage, followed by the prohibition of food, but not water 24 h before the experiment. Caring and treatment of animals were carried out under the supervision of the Research Ethical Committee of Faculty of Pharmacy, Beni-Suef University. Around 3mLwater/rat was given

through gastric inoculation to diminish the edema response variability. The tested compounds **9a-f**, **11a-f** and celecoxib were dissolved in 10% DMSO aqueous solution and then treated orally to the groups at a dose of 50 mg/kg body weight. Coinciding with an injection of 10% DMSO aqueous solution (v/v) into the control group of the rats. After 1 h, the animals were injected by 100 µL of freshly prepared 1% carrageenan-sodium gel (sigma-aldrich, USA), into the sub-planter region of the right hind paw for induction of paw edema. Vernier caliper (SMIEC) was used to measure the right and left hind paw of each rat immediately after 1, 3 and 5 h of induction of inflammation. The left hind paw was exploited as a control for determining the intensity of the inflammation in the right hind paw. The proportion of anti-inflammatory activity was outlined by calculating the reduction in edema thickness induced by carrageenan.

4.2.2.3. Cardiovascular Evaluation:

The experiments were carried out on adult male albino Wister rats (170-200 g) obtained from animal house, Nahda University, Beni-Suef as previously reported [51,52]. The animals were split into four groups with six animals in each one after housing at controlled temperature 25±2˚C with normal light/dark cycles, where the applied protocol of caring and treatment was approved by the Research Ethical Committee of Faculty of Pharmacy, Beni-Suef University, which is a member of the Egyptian Network of Research Ethics Committees (ENREC) and which followed the recommendations of the National Institutes of Health (NIH) Guide for Care and Use of Laboratory Animals (NIH Publication No. 8023, revised 1978). A suspension of the tested compounds **9b**, **9c** and celecoxib in 1% tween in saline was given orally to the groups at a dose 100mg/kg body weight. Only one group received saline to act as a control group. Administration of the drugs was continued for 2 weeks and, on the 15^{th} day, collection of the blood samples from the retro-orbital plexus vein of all rats were executed. The clotting of the blood samples was carried out at room temperature followed by centrifugation at 1500 rpm for 10 min for serum separation. Storage of the serum samples were performed at -20 ^{o}C for analysis of LDH, CK-MB, TNF-α and cTn-I [67]. Subsequently, the animals were sacrificed via cervical dislocation and cautiously dissected. The hearts were exposed through making an incision

along the thorax followed by washing with ice-cold normal saline solution and dried with filter papers. Afterward, the homogenized hearts were obtained using a homogenizer to prepare 25% w/v homogenate in ice-cooled saline followed by centrifugation at 2000 rpm for 20 min at 4^{o}C, then stored at -80^{o}C for supplementary biochemical analysis of GSH. For the histopathological study, hearts were kept in 10% formal saline.

Rat Cardiac Troponin-I (cTn-I) ELISA kit was supplied by CusaBio, USA, with Catalog number CSB-E08594r, detection range 31.25–2000 pg/ml, detection wavelength 450 nm, inter-assay variability 10%, and intra-assay variability 8%. Tumor necrosis factor- alpha (TNF-α) ELISA kits was obtained from Ray Biotech, USA (Catalog number ELRTNFalpha-001C, detection range 25–20,000 pg/ml, detection wavelength 450 nm, inter- and intra-assay variability are lower than 10% and inter-assay variability 12%). Prostacyclin (PGI_2) ELISA Kit (OKEH02555) Lot# KC2119 was supplied by Aviva Systems Biology, Corp. San Diego, USA. Detection range 31.2–2000 pg/ml, detection wavelength of 450 nm. Lactate dehydrogenase (LDH) kit was purchased from SPINREACT S.A.U. Spain. Detection wavelength of 340 nm. Creatine kinase-MB (CK-MB) was obtained from SPINREACT S.A.U. Spain. Detection wavelength 340 nm. All other chemicals and reagents used were of analytical grade while celecoxib purchased as Celebrex 100 mg capsule.

The biochemical parameters were assayed as following; Troponin-I (cTn-I)), Tumor necrosis factor-α (TNF-α), and Prostacyclin (PGI_2) were measured in serum using ELISA kits according to the reported method [68–70]. While LDH and CK-MB levels were determined spectrophotometry according to reported procedures [71,72]. The oxidative stress markers GSH was assessed in heart homogenates by chemical methods, as previously described [73].

On the other hand, the histo-pathological study was carried out after solidification of the dried hearts in 10% formalin solution in saline for subsequent preparation of paraffin sections. Routine hematoxylin and eosin (H&E) stain was used as mentioned previously [74,75].

4.4. Physicochemical parameters:

Physicochemical parameters of all the compounds were predicted computationally using the Molinspiration online property calculation toolkit [63]. All the obtained results were outlined in **Table 4** expect for the percentage of absorption (%ABS) that has been calculated according to the following equation %ABS = 109 - (0.345 × tPSA) [64].

Acknowledgments:

The authors thank the confirmatory diagnostic unit at Egyptian Company for Drugs and Veterinary Vaccines (*VACSERA*) for performing some of the *in vitro* biological tests.

References:

[1] A.H. Abdelazeem, S.I. Khan, S.W. White, K.J. Sufka, C.R. Mccurdy, Design, Synthesis and Biological Evaluation of Bivalent Benzoxazolone and Benzothiazolone Ligands as Potential Anti- inflammatory/Analgesic Agents, Bioorganic and Medicinal Chemistry. 23 (2015) 3248–3259. https://doi.org/10.1016/j.bmc.2015.04.057.Design.

[2] M.H. Abdelrahman, B.G.M. Youssif, M.A. abdelgawad, A.H. Abdelazeem, H.M. Ibrahim, A.E.G.A. Moustafa, L. Treamblu, S.N.A. Bukhari, Synthesis, biological evaluation, docking study and ulcerogenicity profiling of some novel quinoline-2-carboxamides as dual COXs/LOX inhibitors endowed with anti-inflammatory activity, European Journal of Medicinal Chemistry. 127 (2017) 972–985. https://doi.org/10.1016/j.ejmech.2016.11.006.

[3] N.H. Amin, A.A. Mohammed, K.R.A. Abdellatif, Novel 4-methylsulfonylphenyl derivatives as NSAIDS with preferential COX-2 inhibition, Future Medicinal Chemistry. 10 (2018) 53–70. https://doi.org/10.4155/fmc-2017-0153.

[4] A.J. Higgins, P. LEES, The acute inflammatory process, arachidonic acid metabolism and the mode of action of anti-inflammatory drugs, Equine Veterinary Journal. 16 (1984) 163–175. https://doi.org/10.1111/j.2042-3306.1984.tb01893.x.

[5] R. Hammamieh, M. Jett, Potential roles for inhibitors of arachidonic acid metabolism in prevention and treatment of breast cancer, Future Lipidology. 3 (2008) 265–271. https://doi.org/10.2217/17460875.3.3.265.

[6] A.H. Abdelazeem, M.T. El-Saadi, E.G. Said, B.G.M. Youssif, H.A. Omar, S.M. El-Moghazy, Novel diphenylthiazole derivatives with multi-target mechanism: Synthesis, docking study, anticancer and anti-inflammatory activities, Bioorganic Chemistry. 75 (2017) 127–138. https://doi.org/10.1016/j.bioorg.2017.09.009.

[7] A.H. Abdelazeem, S.A. Abdelatef, M.T. El-Saadi, H.A. Omar, S.I. Khan, C.R. McCurdy, S.M. El-Moghazy, Novel pyrazolopyrimidine derivatives targeting COXs and iNOS enzymes; Design, synthesis and biological evaluation as potential anti-inflammatory agents, European Journal of Pharmaceutical Sciences. 62 (2014) 197–211. https://doi.org/10.1016/j.ejps.2014.05.025.

[8] P. Srivastava, V.K. Vyas, B. Variya, P. Patel, G. Qureshi, M. Ghate, Synthesis, anti-inflammatory, analgesic, 5-lipoxygenase (5-LOX) inhibition activities, and molecular docking study of 7-substituted coumarin derivatives, Bioorganic Chemistry. 67 (2016) 130–138. https://doi.org/10.1016/j.bioorg.2016.06.004.

[9] E.A. Dennis, J. Cao, Y. Hsu, V. Magrioti, G. Kokotos, Phospholipase A enzymes Physical Structure, Biological Function, Chemical Reviews. 111 (2011) 6130–6185.

[10] B. Waltenberger, U. Garscha, V. Temml, J. Liers, O. Werz, D. Schuster, H. Stuppner, Discovery of Potent Soluble Epoxide Hydrolase (sEH) Inhibitors by Pharmacophore-Based Virtual Screening, Journal of Chemical Information and Modeling. 56 (2016) 747–762. https://doi.org/10.1021/acs.jcim.5b00592.

[11] K. Meirer, D. Steinhilber, E. Proschak, Inhibitors of the arachidonic acid cascade: Interfering with multiple pathways, Basic and Clinical Pharmacology and Toxicology. 114 (2014) 83–91. https://doi.org/10.1111/bcpt.12134.

[12] R. Gautam, S.M. Jachak, Recent Developments in Anti- Inflammatory Natural Products, Medicinal Research Reviews. 29 (2009) 767–820. https://doi.org/10.1002/med.

[13] G.A. Green, Understanding NSAIDs: From aspirin to COX-2, Clinical Cornerstone. 3 (2001) 50–59. https://doi.org/10.1016/S1098-3597(01)90069-9.

[14] C.D. Poff, M. Balazy, Drugs that target lipoxygenases and leukotrienes as emerging therapies for asthma and cancer, Current Drug Targets: Inflammation and Allergy. 3 (2004) 19–33. https://doi.org/10.2174/1568010043483917.

[15] D. Wang, R.N. Dubois, Prostaglandins and cancer, Gut. 55 (2006) 115–122.

[16] F. Buttgereit, G.R. Burmester, L.S. Simon, Gastrointestinal toxic side effects of nonsteroidal anti-inflammatory drugs and cyclooxygenase-2-specific inhibitors, American Journal of Medicine. 110 (2001) 13–19. https://doi.org/10.1016/s0002-9343(00)00728-2.

[17] E. Ortiz, Market withdrawal of Vioxx: is it time to rethink the use of COX-2 inhibitors?, Journal of Managed Care Pharmacy : JMCP. 10 (2004) 551–554.

[18] X. Ding, P.A. Murray, Cellular mechanisms of thromboxane A2-mediated contraction in pulmonary veins, American Journal of Physiology - Lung Cellular and Molecular Physiology. 289 (2005) 825–833. https://doi.org/10.1152/ajplung.00177.2005.

[19] J. Kermode, W. Butt, F. Shann, Comparison between prostaglandin E1 and epoprostenol (prostacyclin) in infants after heart surgery, British Heart Journal. 66 (1991) 175–178. https://doi.org/10.1136/hrt.66.2.175.

[20] A. Iyer, K. Kauter, M.A. Alam, S.H. Hwang, C. Morisseau, B.D. Hammock, L. Brown, Pharmacological inhibition of soluble epoxide hydrolase ameliorates diet-induced metabolic syndrome in rats, Experimental Diabetes Research. 2012 (2012) 14–16. https://doi.org/10.1155/2012/758614.

[21] J.H. Capdevila, J.R. Falck, R.C. Harris, Cytochrome P450 and arachidonic acid bioactivation: Molecular and functional properties of the arachidonate monooxygenase, Journal of Lipid Research. 41 (2000) 163–181.

[22] K. Node, Y. Huo, X. Ruan, B. Yang, M. Spiecker, K. Ley, D.C. Zeldin, J.K. Liao, Anti-inflammatory properties of cytochrome P450 epoxygenase-derived eicosanoids, Science. 285 (1999) 1276–1279. https://doi.org/10.1126/science.285.5431.1276.

[23] Y. Liu, Y. Zhang, K. Schmelzer, T.S. Lee, X. Fang, Y. Zhu, A.A. Spector, S. Gill, C. Morisseau, B.D. Hammock, J.Y.J. Shyy, The antiinflammatory effect of laminar flow: The role of PPARγ, epoxyeicosatrienoic acids, and soluble epoxide hydrolase, Proceedings of the National Academy of Sciences of the United States of America. 102 (2005) 16747–16752. https://doi.org/10.1073/pnas.0508081102.

[24] B. Inceoglua, S.L. Jinksb, K.R. Schmelzera, T. Waitea, I.H. Kima, B.D. Hammock, Inhibition of soluble epoxide hydrolase reduces LPS-induced thermal hyperalgesia

and mechanical allodynia in a rat model of inflammatory pain, Life Science Journal. 79 (2006) 2311–2319.

[25] B. Inceoglu, S.L. Jinks, A. Ulu, C.M. Hegedus, K. Georgi, K.R. Schmelzer, K. Wagner, P.D. Jones, C. Morisseau, B.D. Hammock, Soluble epoxide hydrolase and epoxyeicosatrienoic acids modulate two distinct analgesic pathways, Proceedings of the National Academy of Sciences of the United States of America. 105 (2008) 18901–18906. https://doi.org/10.1073/pnas.0809765105.

[26] W.B. Campbell, I. Fleming, Epoxyeicosatrienoic acids and endothelium-dependent responses, Pflugers Archiv European Journal of Physiology. 459 (2010) 881–895. https://doi.org/10.1007/s00424-010-0804-6.

[27] N. Chiamvimonvat, C.M. Ho, H.J. Tsai, B.D. Hammock, The soluble epoxide hydrolase as a pharmaceutical target for hypertension, Journal of Cardiovascular Pharmacology. 50 (2007) 225–237. https://doi.org/10.1097/FJC.0b013e3181506445.

[28] R.J. Roman, P -450 Metabolites of Arachidonic Acid in the Control of Cardiovascular Function , Physiological Reviews. 82 (2002) 131–185. https://doi.org/10.1152/physrev.00021.2001.

[29] J.D. Imig, Epoxides and Soluble Epoxide Hydrolase in Cardiovascular Physiology John, Physiological Reviews. 92 (2012) 101–130. https://doi.org/10.1038/jid.2014.371.

[30] A.A. Quyyumi, M. Ozkor, Vasodilation by hyperpolarization: Beyond NO, Hypertension. 48 (2006) 1023–1025. https://doi.org/10.1161/01.HYP.0000250965.03934.15.

[31] D.Y. Xu, B.B. Davis, Z.H. Wang, S.P. Zhao, B. Wasti, Z.L. Liu, N. Li, C. Morisseau, N. Chiamvimonvat, B.D. Hammock, A potent soluble epoxide hydrolase inhibitor, t-AUCB, acts through PPARγ to modulate the function of endothelial progenitor cells from patients with acute myocardial infarction, International Journal of Cardiology. 167 (2013) 1298–1304. https://doi.org/10.1016/j.ijcard.2012.03.167.

[32] J.D. Imig, Epoxyeicosatrienoic Acids and 20-Hydroxyeicosatetraenoic Acid on Endothelial and Vascular Function, Advances in Pharmacology, (77) 2016. https://doi.org/10.1016/bs.apha.2016.04.003.

[33] M. Revermann, E. Barbosa-Sicard, E. Dony, R.T. Schermuly, C. Morisseau, G. Geisslinger, I. Fleming, B.D. Hammock, R.P. Brandes, Inhibition of the soluble epoxide hydrolase attenuates monocrotaline- induced pulmonary hypertension in rats, Journal of Hypertension. 27 (2009) 322–331. https://doi.org/10.1097/HJH.0b013e32831aedfa.

[34] A. Ulu, B.B. Davis, H.-J. Tsai, I.-H. Kim, C. Morisseau, B. Inceoglu, O. Fiehn, B.D. Hammock, and R.H. Weiss., Soluble Epoxide Hydrolase Inhibitors Reduce the Development of Atherosclerosis in Apolipoprotein E-Knockout Mouse Model, Journal of Cardiovascular Pharmacology. 52 (2008) 314–323. https://doi.org/10.1038/jid.2014.371.

[35] S. Ghosh, P.C. Chiang, J.L. Wahlstrom, H. Fujiwara, J.G. Selbo, S.L. Roberds, Oral delivery of 1,3-dicyclohexylurea nanosuspension enhances exposure and lowers blood pressure in hypertensive rats, Basic and Clinical Pharmacology and Toxicology. 102 (2008) 453–458. https://doi.org/10.1111/j.1742-7843.2008.00213.x.

[36] J.D. Imig, Epoxide hydrolase and epoxygenase metabolites as therapeutic targets for renal diseases, American Journal of Physiology - Renal Physiology. 289 (2005) 496–503. https://doi.org/10.1152/ajprenal.00350.2004.

[37] J.D. Imig, X. Zhao, J.H. Capdevila, C. Morisseau, B.D. Hammock, Soluble epoxide hydrolase inhibition lowers arterial blood pressure in angiotensin II hypertension, Hypertension. 39 (2002) 690–694. https://doi.org/10.1161/hy0202.103788.

[38] L. Yang, J. Cheriyan, D.D. Gutterman, R.J. Mayer, Z. Ament, J.L. Griffin, A.L. Lazaar, D.E. Newby, R. Tal-Singer, I.B. Wilkinson, Mechanisms of Vascular Dysfunction in COPD and Effects of a Novel Soluble Epoxide Hydrolase Inhibitor in Smokers, Chest. 151 (2017) 555–563. https://doi.org/10.1016/j.chest.2016.10.058.

[39] A.L. Lazaar, L. Yang, R.L. Boardley, N.S. Goyal, J. Robertson, S.J. Baldwin, D.E. Newby, I.B. Wilkinson, R. Tal-singer, R.J. Mayer, J. Cheriyan, Pharmacokinetics, pharmacodynamics and adverse event profile of GSK2256294, a novel soluble epoxide hydrolase inhibitor, British Journal of Clinical Pharmacology. 81 (2015) 971–979. https://doi.org/10.1111/bcp.12855.

[40] H.C. Shen, B.D. Hammock, Discovery of Inhibitors of Soluble Epoxide Hydrolase : A Target with Multiple Potential Therapeutic Indications, Journal of Medicinal

[41] K.R. Schmelzer, B. Inceoglu, L. Kubala, I.H. Kim, S.L. Jinks, J.P. Eiserich, B.D. Hammock, Enhancement of antinociception by coadministration of nonsteroidal anti-inflammatory drugs and soluble epoxide hydrolase inhibitors, Proceedings of the National Academy of Sciences of the United States of America. 103 (2006) 13646–13651. https://doi.org/10.1073/pnas.0605908103.

[42] J.D. Imig, B.D. Hammock, Soluble epoxide hydrolase as a therapeutic target for cardiovascular diseases, Nature Reviews| Drug Discovery. 8 (2009) 794–805. https://doi.org/10.1038/nrd2875.

[43] A. Chakraborti, S. Garg, R. Kumar, H. Motiwala, P. Jadhavar, Progress in COX-2 Inhibitors: A Journey So Far, Current Medicinal Chemistry. 17 (2010) 1563–1593. https://doi.org/10.2174/092986710790979980.

[44] S. Sidique, R. Ardecky, Y. Su, S. Narisawa, B. Brown, J.L. Millán, E. Sergienko, N.D.P. Cosford, Design and synthesis of pyrazole derivatives as potent and selective inhibitors of tissue-nonspecific alkaline phosphatase (TNAP), Bioorganic and Medicinal Chemistry Letters. 19 (2009) 222–225. https://doi.org/10.1016/j.bmcl.2008.10.107.

[45] N. Bechmann, T. Kniess, M. Köckerling, A. Pigorsch, J. Steinbach, J. Pietzsch, Novel (pyrazolyl)benzenesulfonamides with a nitric oxide-releasing moiety as selective cyclooxygenase-2 inhibitors, Bioorganic and Medicinal Chemistry Letters. 25 (2015) 3295–3300. https://doi.org/10.1016/j.bmcl.2015.05.059.

[46] J.-Y. Yoon, S. Lee, H. Shin, Recent Advances in the Regioselective Synthesis of Pyrazoles, Current Organic Chemistry. 15 (2011) 657–674. https://doi.org/10.2174/138527211794519005.

[47] H.S. Ibrahim, S.M. Abou-Seri, M. Tanc, M.M. Elaasser, H.A. Abdel-Aziz, C.T. Supuran, Isatin-pyrazole benzenesulfonamide hybrids potently inhibit tumor-associated carbonic anhydrase isoforms IX and XII, European Journal of Medicinal Chemistry. 103 (2015) 583–593. https://doi.org/10.1016/j.ejmech.2015.09.021.

[48] S.H. Hwang, K.M. Wagner, C. Morisseau, J. Liu, H. Dong, A.T. Wecksler, B.D. Hammock, Synthesis and Structure À Activity Relationship Studies of Urea-Containing Pyrazoles as Dual Inhibitors of Cyclooxygenase-2 and Soluble Epoxide Hydrolase, Journal of Medicinal Chemistry. (2011) 3037–3050.

[49] D.B.E.J. Koster R., Anderson M., acetic acid for analgesic screening, Federation Proceedings. 18 (1959) 412.

[50] C.A. Winte, E.A. Risley, G.W. Nuss, Carrageenin-Induced Edema in Hind Paw of the 'Rat as an Assay for Antiinflammatory Dkugp., Proceedings of the Society for Experimental Biology and Medicine. 111 (1962) 544–547.

[51] S. Ahmad, B. Prasad, K. Kohli, M. Fahim, K. Dubey, Folic acid ameliorates celecoxib cardiotoxicity in a doxorubicin heart failure rat model, Pharmaceutical Biology. 55 (2017) 1295–1303. https://doi.org/10.1080/13880209.2017.1299768.

[52] S. Ahmad, B. Prasad, M. Fahim, N. Dhyani, K. Dubey, Ameliorative Effect of Beraprost Sodium on Celecoxib Induced Cardiotoxicity in Rats, Iranian Journal of Pharmaceutical Research. 17 (2018) 155–163.

[53] A.G. Olatidoye, A.H.B. Wu, Y.-J. Feng, D. Waters, Prognostic Role of Troponin T Versus Troponin I in Unstable Angina Pectoris for Cardiac Events With Meta-Analysis Comparing Published Studies, The American Journal of Cardiology. 9149 (1998) 1405–1410.

[54] K.H.S. Farvin, R. Anandan, S.H. Senthil, K.S. Shiny, T. V Sankar, T.K. Thankappan, Effect of squalene on tissue defense system in isoproterenol-induced myocardial infarction in rats, Pharmacological Research. 50 (2004) 231–236. https://doi.org/10.1016/j.phrs.2004.03.004.

[55] T. Tsutamoto, C. Kawahara, K. Nishiyama, M. Yamaji, Prognostic role of highly sensitive cardiac troponin I in patients with systolic heart failure, American Heart Journal. 159 (2010) 63–67. https://doi.org/10.1016/j.ahj.2009.10.022.

[56] Q. Zhou, X. Pan, L. Wang, X. Wang, D. Xiong, The protective role of neuregulin-1 : A potential therapy for sepsis-induced cardiomyopathy, European Journal of Pharmacology. 788 (2016) 234–240. https://doi.org/10.1016/j.ejphar.2016.06.042.

[57] S. Gupta, P. Sarotra, R. Aggarwal, Role of Oxidative Stress in Celecoxib-Induced Renal Damage in Wistar Rats, Digestive Diseases and Sciences. (2007) 3092–3098. https://doi.org/10.1007/s10620-007-9788-2.

[58] M. S, V. JR., The role of prostacyclin in vascular tissue., Federation Proceedings. 1 (1979) 66–71.

[59] G.A. Gomez, Human soluble epoxide hydrolase: Structural basis of inhibition by 4-(3-cyclohexylureido)-carboxylic acids, Protein Science. 15 (2006) 58–64.

[60] G.A. Gomez, C. Morisseau, B.D. Hammock, D.W. Christianson, Structure of Human Epoxide Hydrolase Reveals Mechanistic Inferences on Bifunctional Catalysis in Epoxide and Phosphate Ester Hydrolysis, Biochemistry. 43 (2004) 4716–4723. https://doi.org/10.1021/bi036189j.

[61] Y. Kato, N. Fuchi, H. Saburi, Y. Nishimura, A. Watanabe, M. Yagi, Y. Nakadera, E. Higashi, M. Yamada, T. Aoki, Discovery of 2,8-diazaspiro[4.5]decane-based trisubstituted urea derivatives as highly potent soluble epoxide hydrolase inhibitors and orally active drug candidates for treating hypertension, Bioorganic and Medicinal Chemistry Letters. 23 (2013) 5975–5979. https://doi.org/10.1016/j.bmcl.2013.08.054.

[62] C.A. Lipinski, F. Lombardo, B.W. Dominy, P.J. Feeney, Experimental and computational approaches to estimate solubility and permeability in drug discovery and development settings, Advanced Drug Delivery Reviews. 64 (2012) 4–17. https://doi.org/10.1016/j.addr.2012.09.019.

[63] Molinspiration Cheminformatics www.molinspiration.com/services/properties.html, (n.d.).

[64] Y.H. Zhao, M.H. Abraham, J. Le, A. Hersey, C.N. Luscombe, G. Beck, B. Sherborne, I. Cooper, Rate-limited steps of human oral absorption and QSAR studies, Pharmaceutical Research. 19 (2002) 1446–1457. https://doi.org/10.1023/A:1020444330011.

[65] M.S. Mohamed, Y.E. Mansour, H.K. Amin, M.E. El-Araby, Molecular modelling insights into a physiologically favourable approach to eicosanoid biosynthesis inhibition through novel thieno[2,3-b]pyridine derivatives, Journal of Enzyme Inhibition and Medicinal Chemistry. 33 (2018) 755–767. https://doi.org/10.1080/14756366.2018.1457657.

[66] X.Y. Lu, Z.C. Wang, T. Wei, X.Q. Yan, P.F. Wang, H.L. Zhu, Design, synthesis and evaluation of benzenesulfonamide-substituted 1,5-diarylpyrazoles containing phenylacetohydrazide derivatives as COX-1/COX-2 agents against solid tumors, RSC Advances. 6 (2016) 22917–22935. https://doi.org/10.1039/c6ra02168a.

[67] N.R. Locke, S.G. Royce, J.S. Wainewright, C.S. Samuel, M.L. Tang, Comparison of Airway Remodeling in Acute , Subacute , and Chronic Models of Allergic

Airways Disease, American Journal Of Respiratory Cell and Molecular Biology. 36 (2007) 625–632. https://doi.org/10.1165/rcmb.2006-0083OC.

[68] A. Corti, C. Poiesi, S. Merli, G. Cassani, Tumor necrosis factor (TNF) a quantification by ELISA and bioassay : effects of TNF -soluble TNF receptor (p55) complex dissociation during assay incubations, Journal of Immunological Methods. 1 (1994) 191–198.

[69] H.A. Katus, A. Remppis, S. Looser, K. Hallemeier, T. Scheffold, W. Kiibler, Enzyme Linked Immune of Acute Assay of Cardiac Troponin T for the Myocardial Infarction in Patients, Journal of Molecular and Cellular Cardiology. 353 (1989) 1349–1353.

[70] J.C. Docherty, J.M. Gerrard, An Enzyme-linked Immunosorbent Assay For 6-Keto PGF alfa, Prostaglandins. 31 (1986) 375–383.

[71] P.S. Rao, J.J. Lukes, S.M.H. Ayres andMueller, New manual and automated method for determining activity of creatine kinase isoenzyme MB, by use of dithiothreitol: clinical applications, Clinical Chemistry. 21 (1975) 1612–1618.

[72] R.G. Martinek, A Rapid Ultraviolet Spectrophotometric Lactic Dehydrogenase Assay, Clinica Chimica Acta. 40 (1972) 91–99.

[73] I. Rahman, A. Kode, S.K. Biswas, Assay for quantitative determination of glutathione and glutathione disulfide levels using enzymatic recycling method, Nature Protocols. 1 (2006) 3159–3165. https://doi.org/10.1038/nprot.2006.378.

[74] S.R. Kaplan, J.J. Gard, L. Carvajal-huerta, J.C. Ruiz-cabezas, G. Thiene, J.E. Saffitz, Structural and molecular pathology of the heart in Carvajal syndrome, Cardiovascular Pathology. 13 (2004) 26–32. https://doi.org/10.1016/S1054-8807(03)00107-8.

[75] A.H.M.V. Swamy, U.M. Patel, B.C. Koti, P.C. Gadad, N.L. Patel, A.H.M. Thippeswamy, Cardioprotective effect of Saraca indica against cyclophosphamide induced cardiotoxicity in rats : A biochemical , electrocardiographic and histopathological study, Indian Journal of Pharmacology. 45 (2013) 44–48. https://doi.org/10.4103/0253-7613.106434.

Highlights

1- Two series of 1,5-diarylpyrazole linked to either urea moiety (**9a-f**) or amide moiety (**11a-f)** were synthesized.
2- Novel compounds were evaluated *in vitro* against both COX-2/sEH targets.
3- *In vivo* screening of the anti-inflammatory and analgesic activity for the new synthesized compounds was done.
4- Cardiovascular profile of the most active compounds **9b** and **9c** was examined.
5- Compound **9c** exhibited the most anti-inflammatory/analgesic activity with safe cardiovascular profile.

Declaration of interests

☒ The authors declare that they have no known competing financial interests or personal relationships that could have appeared to influence the work reported in this paper.

☐The authors declare the following financial interests/personal relationships which may be considered as potential competing interests: